SOME FACTORS INFLUENCING FLOW CHARACTERISTICS OF A TWO-DIMENSIONAL EXPANSION

by

Steven M. Hindall

A Thesis Submitted to the Faculty of the

DEPARTMENT OF CIVIL ENGINEERING

In Partial Fulfillment of the Requirements
For the Degree of

MASTER OF SCIENCE

In the Graduate College

THE UNIVERSITY OF ARIZONA

1 9 6 6

STATEMENT BY AUTHOR

This thesis has been submitted in partial fulfillment of requirements for an advancd degree at The University of Arizona and is deposited in the University Library to be made available to borrowers under rules of the Library.

Brief quotations from this thesis are allowable without special permission provided that accurate acknowledgment of the source is made. Requests for permission for extended manuscript in whole or in part may be granted by the head of the major department or the dean of the graduate college when in his judgment the proposed use of the material is in the interest of scholarship. In all other instances, however, permission must be obtained from the author.

SIGNED: Steven M Hindall

APPROVAL BY THESIS DIRECTOR

This thesis has been approved on the date shown below:

Thomas Carmody — May 6, 1966

THOMAS CARMODY
Assistant Professor of
Civil Engineering

Date

ACKNOWLEDGMENTS

The direction and assistance given the writer by Dr. Thomas Carmody, thesis director, and by my colleague, Bruce Ward, are greatly appreciated.

The assistance and suggestions given by Mr. Brooks Muterspaugh and Mr. Louis Gemson, technicians for the Department of Civil Engineering, have been invaluable.

To my wife, Sandy, I can only say thanks for understanding, encouragement, and sacrifices.

TABLE OF CONTENTS

		Page
LIST OF ILLUSTRATIONS		v
LIST OF TABLES		v
CHAPTER		
1	INTRODUCTION	1
2	STATEMENT OF THE PROBLEM	4
3	METHOD OF ANALYSIS	6
	3.1 Momentum Analysis	10
	3.2 Energy Analysis	12
4	EXPERIMENTAL PHASE	14
	4.1 Apparatus	14
	4.2 Procedure	16
	4.3 Evaluation of Data	20
	4.4 Experimental Results	23
	4.5 Interpretation of Results	29
5	CONCLUSIONS AND RECOMMENDATIONS	32
	5.1 Conclusions	32
	5.2 Recommendations	38
APPENDIX		39
REFERENCES		59

LIST OF ILLUSTRATIONS

Figure Number	Title	Page
1	Neutral Stability	3
2	Definition Sketch	8
3	Apparatus	17
4	Flow Measuring Instruments	17
5	Apparatus	18
6	Continuity Quantities	26
7	Momentum Quantities	27
8	Energy Dissipation Rates	28
9	Sample Data Sheet	41
10	Pressure Distribution Diagrams	42
11	Centerline Ambient Pressure	43
12	Velocity Distribution Diagrams	44
13	Velocity Distribution Diagrams	45
14	Velocity Distribution Diagrams	46
15	Velocity Distribution Diagrams	47
16	Continuity and Momentum Distributions (Vertical)	48
17	Flow Diagrams	49

LIST OF ILLUSTRATIONS--Continued

Figure Number		Page
18	Flow Diagrams	50
19	Flow Diagrams	51
20	Flow Diagrams	52
21	Flow Diagrams	53
22	Flow Diagrams	54
23	Flow Diagrams	55
24	Flow Diagrams	56
25	Separation Pocket Location	57

LIST OF TABLES

Table Number		Page
1	Nomenclature	9

ABSTRACT

Some stability criteria and loss coefficients for a two-dimensional expansion were determined through the use of continuity, momentum and energy relationships.

A 90-feet-per-second low-turbulence stream of air issuing from a 1 x 10 slot into an expanded rectangular conduit of variable with and degree of symmetry was studied. ($R \doteq 7 \times 10^4$)

Ambient and stagnation pressures were measured in the flow and from these the discharge rates, momentum flux, and energy dissipation rates were determined.

The results clearly indicate that for a stable jet the flow can be analyzed two-dimensionally, while for a neutrally stable jet the flow must be analyzed three-dimensionally. They also point out that both stability and the loss coefficients depend upon the downstream wall spacing ratio.

CHAPTER 1

INTRODUCTION

This paper deals with some factors influencing the characteristics of steady flow through two-dimensional expansions. Of primary concern is the effect of the expansion ratio on the symmetry of the flow pattern. Also of interest is the degree of geometric asymmetry required to produce a significantly asymmetric flow pattern.

The study was performed in a two-dimensional air tunnel with low-turbulence air of a uniform velocity approaching an expansion through a vertical slot. The ratio of downstream width to slot width was varied, and the degree of asymmetry of the wing walls was also varied. Distributions of mean ambient pressure and mean velocity were determined along the horizontal plane through the centerline in all cases and, in addition, at the vertical quarter points for one case. The analysis was performed by evaluating continuity, momentum, and energy relations.

Flow in two-dimensional expansions as shown by the experiment is symmetric and stable until a certain

ratio of slot width to downstream width is reached, beyond which it exists in a condition of neutral stability.

Neutral stability, as illustrated by Figure 1, infers that beyond a certain width ratio the flow tends to concentrate on one side of the centerline or the other with no way to predict the location of the flow concentration; upon changing positions, the flow becomes practically a mirror image of the previous flow. For this location change to take place under neutrally stable conditions, an extraneous external force must be applied in some manner.

NEUTRAL STABILITY

(EXPLANATION)

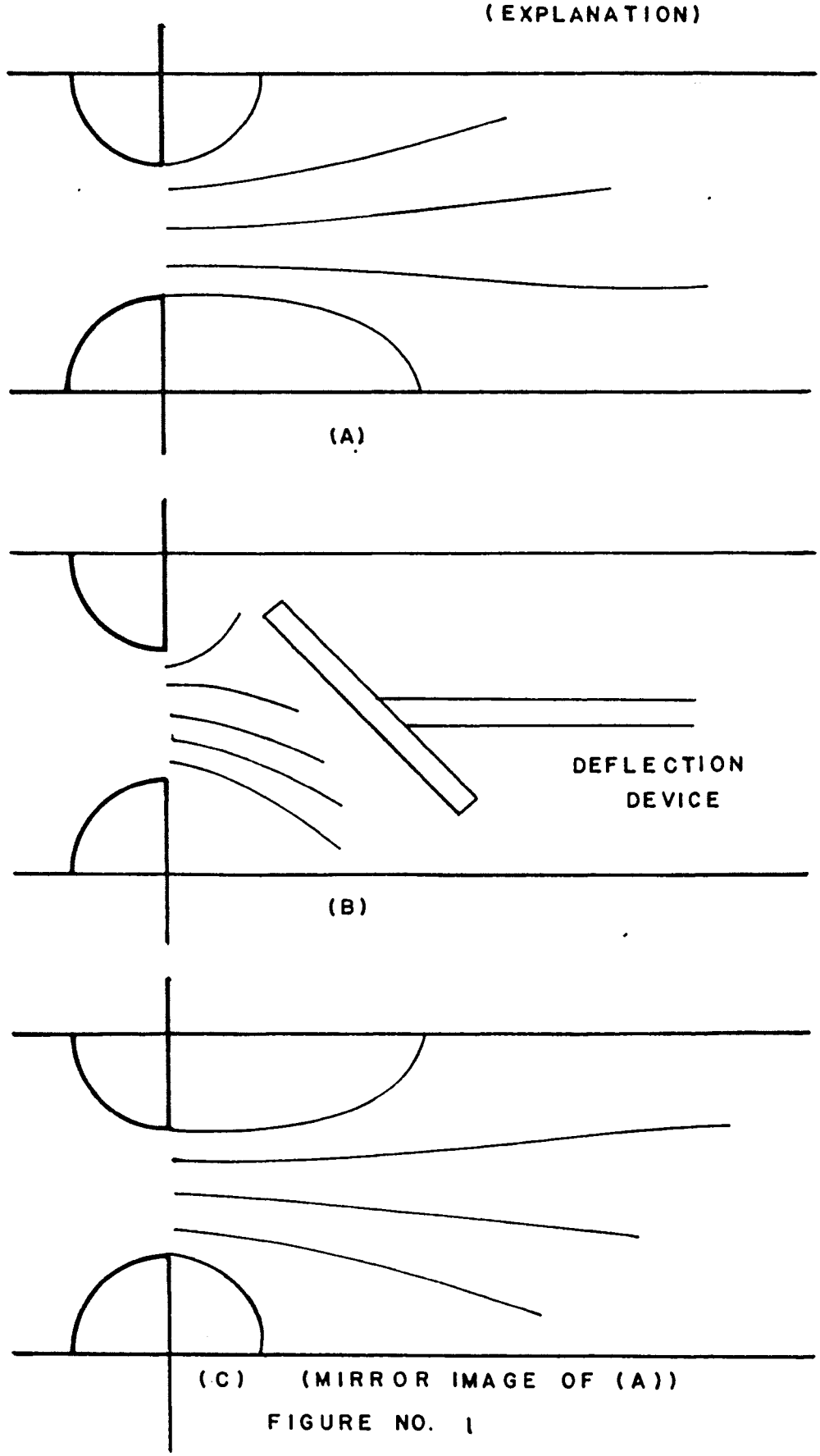

FIGURE NO. 1

CHAPTER 2

STATEMENT OF THE PROBLEM

A submerged jet leaving a confined expansion may behave in three different ways: It may exist in a state of stable equilibrium, a state of neutral equilibrium, or a state of unstable equilibrium. The state of stable equilibrium would be characterized by a single flow pattern which for a symmetric boundary would be expected to produce symmetric flow conditions. The state of neutral equilibrium would be characterized by more than one flow pattern; any of which would seemingly be stable, but the particular pattern existing would be randomly chosen or forced by extraneous means. The state of unstable equilibrium would be characterized by a constantly changing flow pattern.

In any of these cases, the engineer needs to be able to predict flow patterns, pressure distributions and losses in energy. It should be apparent that the stable case should be the most predictable and the unstable case the least predictable. Unfortunately, even the simplest situations have not yet yielded to

analytic treatment except for the infinite field, and then only through rather crude approximations.

The assumptions that have been made in theoretical analyses of jets and wakes in infinite fields have been (1) affine velocity distributions, (2) constant pressure throughout the field, and (3) either a certain form of velocity distribution, or a relationship for the turbulent shear. Since the first two assumptions cannot hold for a finite field, similar theoretical analyses of jets and wakes in finite fields are not at hand.

This study was initiated in order to amass additional experimental evidence concerning two-dimensional jets in finite expansions. The resulting information should be of aid to engineers in predicting flow patterns, both in determining whether the flow will be in stable or neutral equilibrium and in estimating the flow pattern, pressure regain and energy loss.

CHAPTER 3

METHOD OF ANALYSIS

The basic method used in any flow analysis is the examination of continuity, momentum, and energy relationships. These are obtainable directly from analyses of velocity and pressure distributions.

From the velocity distributions it can be determined whether or not a concentration of flow is present at any location. The continuity relation is a check on the accuracy of the measured velocity distribution. By analyzing the results of the momentum analysis an additional check on the velocity distribution can be carried out. A loss coefficient indicating the rate of turbulence-energy dissipation is determined through the energy relationship.

The total pressure as measured by a stagnation tube is defined herein as

$$P_T = P_A + \frac{\rho u^2}{2} + \frac{\rho \bar{u}'^2}{2} \qquad (1)$$

By referring to Figure 1 and Table 1, one can see that when equation (1) is divided by $P_o = \frac{\rho U_o^2}{2}$

it takes the dimensionless form

$$\frac{P_T}{P_o} - \frac{P_A}{P_o} = \frac{u^2}{U_o^2} - \frac{\overline{u'^2}}{U_o^2} \qquad (2)$$

If the turbulence term of equation (2) is neglected, the relative longitudinal velocity becomes

$$\frac{u}{U_o} = \sqrt{\frac{P_T}{P_o} - \frac{P_A}{P_o}} \qquad (3)$$

The velocity distributions can be approximated directly from the pressure distributions by this procedure.

By integrating the velocity over the cross-sectional area, the flow through normal cross-sections can be calculated. From continuity requirements the mean flow rate at one station must equal the mean flow rate at all other stations. There may be slight deviation from this in measured results due to the fact that the flow might not be in actuality two-dimensional and the measurements not extensive enough to fully describe the flow pattern.

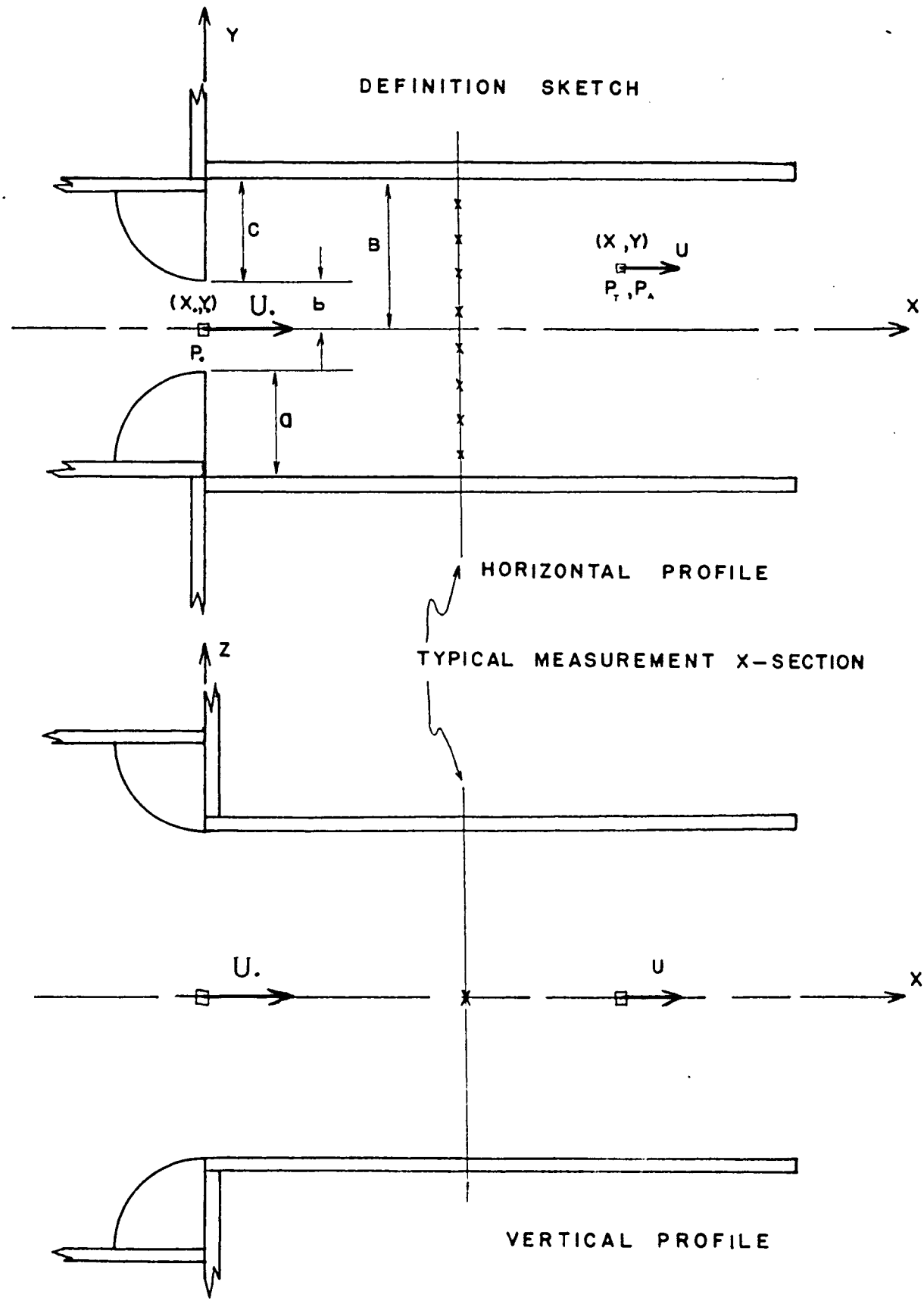
Y
DEFINITION SKETCH
C
B
(X ,Y)
U
P_T ,P_A
(X.,Y.)
U.
b
X
P.
a
HORIZONTAL PROFILE
Z
TYPICAL MEASUREMENT X-SECTION
U.
U
X
VERTICAL PROFILE

FIGURE NO. 2

TABLE 1

Nomenclature

C_l	loss coefficient
D	turbulence-energy dissipation rate
i	free index in tensor notation
j	dummy index in tensor notation
l,m,n	direction cosines
P_A	mean ambient pressure
P_o	free-stream dynamic pressure
P_T	mean total pressure
S	volumetric space of integration
U	slot velocity
U_o	velocity used in the definition of slot dynamic pressure
u,v,w	instantaneous velocity components
$\bar{u},\bar{v},\bar{w}$	temporal-mean velocity components
u',v',w'	instantaneous deviations from temporal-mean velocity components
$\bar{V}$	total mean velocity; $\bar{V}^2$ $\bar{u}^2$ $\bar{v}^2$ $\bar{w}^2$
x,y,z	position coordinates
	mass density of fluid

The general equation governing turbulent flow is the Reynolds equation. It is presented by Rouse[1] on a unit-volume basis in the form

$$\rho \bar{u}_j \frac{\partial \bar{u}_i}{\partial x_j} = \rho X_i - \frac{\partial \bar{p}}{\partial x_i} + \frac{\partial}{\partial x_j}\left(\mu \frac{\partial \bar{u}_i}{\partial x_j} - \rho \overline{u_i' u_j'}\right) \qquad (4)$$

In the x direction, this may be expanded to

$$\rho\left(\bar{u}\frac{\partial \bar{u}}{\partial x} + \bar{v}\frac{\partial \bar{u}}{\partial y} + \bar{w}\frac{\partial \bar{u}}{\partial z}\right) = \rho X - \frac{\partial \bar{p}}{\partial x} + \frac{\partial}{\partial x}\left(\mu \frac{\partial \bar{u}}{\partial x} + \rho \overline{u'u'}\right) + \frac{\partial}{\partial y}\left(\mu \frac{\partial \bar{u}}{\partial y} - \rho \overline{u'v'}\right) + \frac{\partial}{\partial z}\left(\mu \frac{\partial \bar{u}}{\partial z} - \rho \overline{u'w'}\right) \qquad (5)$$

The term on the left signifies the momentum flux. The first term on the right stands for the body forces. The second term represents the pressure force while the third, fourth, and fifth terms are the forces due to the viscous and Reynolds stresses.

By integration of the Reynolds equation and applying Green's theorem to transform certain volume integrals to surface integrals, a more useful form appears, that is, the equation indicating the flux of linear momentum. (See Section 3.1 for further explanation)

3.1 Momentum Analysis

The general equation as found in Rouse[2] is as follows:

$$\rho\int_S n_j u_i u_j\,ds + \rho\int_S n_j \overline{u_i' u_j'}\,ds = \rho\int_{\forall} X_j\,d\forall - \int_S n_i \bar{P}\,ds + \mu\int_S n_j \frac{d\bar{u}_i}{dx_j}\,ds \qquad (6)$$

In the x direction, the general equation may be expanded to

$$\rho\int_S (l\bar{u}^2 + m\bar{u}\bar{v} + n\bar{u}\bar{w})\,ds + \rho\int_S (l\overline{u'^2} + m\overline{u'v'} + n\overline{u'w'})\,ds = \qquad (7)$$

$$\rho\int_{\forall} X\,d\forall - \int_S l\bar{P}\,ds + \mu\int_S \left(l\frac{d\bar{u}}{dx} + m\frac{d\bar{u}}{dy} + n\frac{d\bar{u}}{dz}\right)ds$$

The above equation may be simplified by neglecting the body forces, viscous stresses, and mean transverse velocity components, $\bar{v}$ and $\bar{w}$, reducing Eq. (7) to a simplified two-dimensional momentum-flux equation.

$$\int_{y_1}^{y_2} \rho u^2\,dy + \int_{y_1}^{y_2} P_A\,dy = 0 \qquad (8)$$

Substitution of equation (1) into the above equation yields a form easier to use in calculations,

$$2\int_{y_1}^{y_2} P_T\,dy - \int_{y_1}^{y_2} P_A\,dy = 0 \qquad (9)$$

3.2 Energy Analysis

To obtain the work-energy equation as found in Rouse,[3] the mean and fluctuating components of velocity and pressure, $u_i = \bar{u}_i + \bar{u}_i'$, etc., are substituted for the instantaneous values in the Reynolds equation. If the terms are now averaged, the result will be the differential equation of work and energy.

$$\bar{u}_j \frac{\partial}{\partial x_j}\left(\rho\frac{\bar{V}^2}{2} + \rho\frac{\overline{V'^2}}{2}\right) + \overline{u_j' \frac{\partial(\rho V'^2/2)}{\partial x_j}} + \partial\bar{u}_i \overline{\rho u_i' u_j'} =$$

$$\rho \bar{u}_i x_i - \bar{u}_i \frac{\partial \bar{P}}{\partial x_i} - \mu \bar{u}_j \frac{\partial^2 \bar{u}_i}{\partial x_j \partial x_j} + \mu \overline{u_i' \frac{\partial^2 u_i'}{\partial x_j \partial x_j}} \qquad (10)$$

Upon integrating Eq. (10) over a given region of space, and after the appropriate volume integrals have been changed by the Gaussian theorem to surface integrals, it can be shown that the following work-energy equation emerges.

$$\int_S \rho \frac{\bar{V}^2}{2} \bar{u}_j \frac{\partial x_j}{\partial n} ds + \int_S \bar{u}_i \rho \overline{u_i' u_j'} \frac{\partial x_j}{\partial n} ds -$$

$$\int_\forall \rho \overline{u_i' u_j'} \frac{\partial \bar{u}_i}{\partial x_j} d\forall = \int_\forall \rho \bar{u}_i X \, d\forall +$$

$$\int_S \bar{P} \bar{u}_i \frac{\partial \bar{u}_i}{\partial x_j} ds + \int_S \mu\left(\frac{\partial \bar{u}_i}{\partial x_j} + \frac{\partial \bar{u}_j}{\partial x_i}\right) \bar{u}_i \frac{\partial x_j}{\partial n} ds - \qquad (11)$$

$$\int_\forall \mu\left(\frac{\partial \bar{u}_i}{\partial x_j} + \frac{\partial u_j}{\partial x_i}\right) \frac{\partial \bar{u}_i}{\partial x_j} d\forall$$

The extreme left term represents the net flux of kinetic energy out of the region; the second and third

terms represent the rate at which work is done by the Reynolds stresses over the surface and throughout the interior of the region, respectively. The first and second terms at the right of the equality are the rates at which work is done by the external pressures and body forces. The third and fourth are the rates at which work is done by the viscous stresses.

When the same assumptions used in the momentum analysis are applied to the energy analysis, the following equation is obtained,

$$\int_S \rho \frac{V^2}{2} \bar{u}\, ds - \int_\forall \rho\, \overline{u_i' u_j'} \frac{\partial \bar{u}_i}{\partial x_j}\, d\forall = -\int_S p_A \bar{u}\, ds$$

But $$V \cong \bar{u} \;;$$

and $$\rho \frac{u^2}{2} = p_T - p_A$$

and if one sets

$$D = \int_\forall \rho\, \overline{u_i' u_j'} \frac{d\bar{u}_i}{\partial x_j}\, d\forall$$

the rate of turbulence-energy production within a finite volume may be expressed as

$$D = \int_S \rho \frac{\bar{u}^3}{2}\, dy + \int_S p_A \bar{u}\, dy$$

or

$$D = \int_S p_T \bar{u}\, dy \,. \qquad (12)$$

CHAPTER 4

EXPERIMENTAL PHASE

4.1 Apparatus

The apparatus used for this study consisted of a blower, approach section and contraction, an abrupt expansion, and the instruments used in data collection.

The blower was a two-horsepower centrifugal ventilation blower with a 6 x 11-inch outlet. It was connected to the tunnel with a rubber coupling to reduce vibration. From the blower the tunnel increased in size to 6 x 19 inches and remained this size for a length of 28 inches. At the tunnel exit an offset quarter-round contraction forming a 1 1/2 x 15-inch vertical exit slot was fastened. In the tunnel and the blower there were several vanes and a series of screens to reduce turbulence and to make the flow more nearly irrotational and uniform throughout. The blower, tunnel and contraction were rigidly attached to a steel frame which was mounted on a heavy table. Construction of the tunnel was as follows: one-quarter-inch plywood sides, tops, and bottoms were bolted to welded steel frames. The wood-covered frames bolted together formed the tunnel. There

were no protrusions on the inside of the tunnel to disturb the flow.

The expansion was made of 1/4-inch transparent Plexiglas and consisted of an abutment in the vertical plane mounted on the contraction, two horizontal 18 x 24-inch plywood plates, one installed flush with the bottom of the slot against the abutment, the other flush with the top of the slot, and two vertical 15 x 24-inch wing walls movable to any position up to 18 inches apart, installed perpendicular to the abutment. There were strategically placed wall ambient-pressure taps and 3/8-inch access holes for the pressure probes.

The pressure-probe assembly which was used to hold the different probes and position them in the flow was a T configuration made of 3/8-inch brass pipe, as shown in Figure 4. This assembly was connected by a soft plastic tube to an alcohol precision manometer readable to 0.04 inches.

There were three different pitot-type probes all made of 1/16-inch brass tubing with an inside-to-outside diameter ratio of 0.577. These were a stagnation-pressure probe, an ambient-pressure probe, and a reverse-flow stagnation-pressure probe. The openings were upstream farther than twelve times the diameter of the transverse 3/8-inch brass rod so as not to be affected by it. The

tip of the ambient probe extended 5/8 inch beyond the four circumferentially spaced 0.01-inch sensing holes. This was done to let the flow adjacent to the probe become established before reaching the holes. The end was plugged and rounded to an elliptical shape to keep separation to a minimum. There were also two exploratory probes constructed like the others but used for vertical traversing only.

4.2 Experimental Procedure

The wing walls were placed at the desired spacing to be studied, either symmetric or asymmetric (refer to Fig. 2). All the joints where the pieces fit together were taped to prevent any leakage of flow in the expansion. With this completed, the apparatus was ready for operation.

The specially designed pressure probe was inserted into the flow through holes in the wing walls. Stagnation and ambient pressure readings were taken at 1/4-inch transverse intervals in the horizontal plane along the longitudinal centerline, as shown in Figure 2.

The wing walls were reset at different spacings and the complete procedure repeated.

Before and after each run, the air temperature and stagnation pressure at the expansion were recorded.

COMPLETE APPARATUS

FIGURE NO. 3

INSTRUMENTS

FIGURE NO. 4

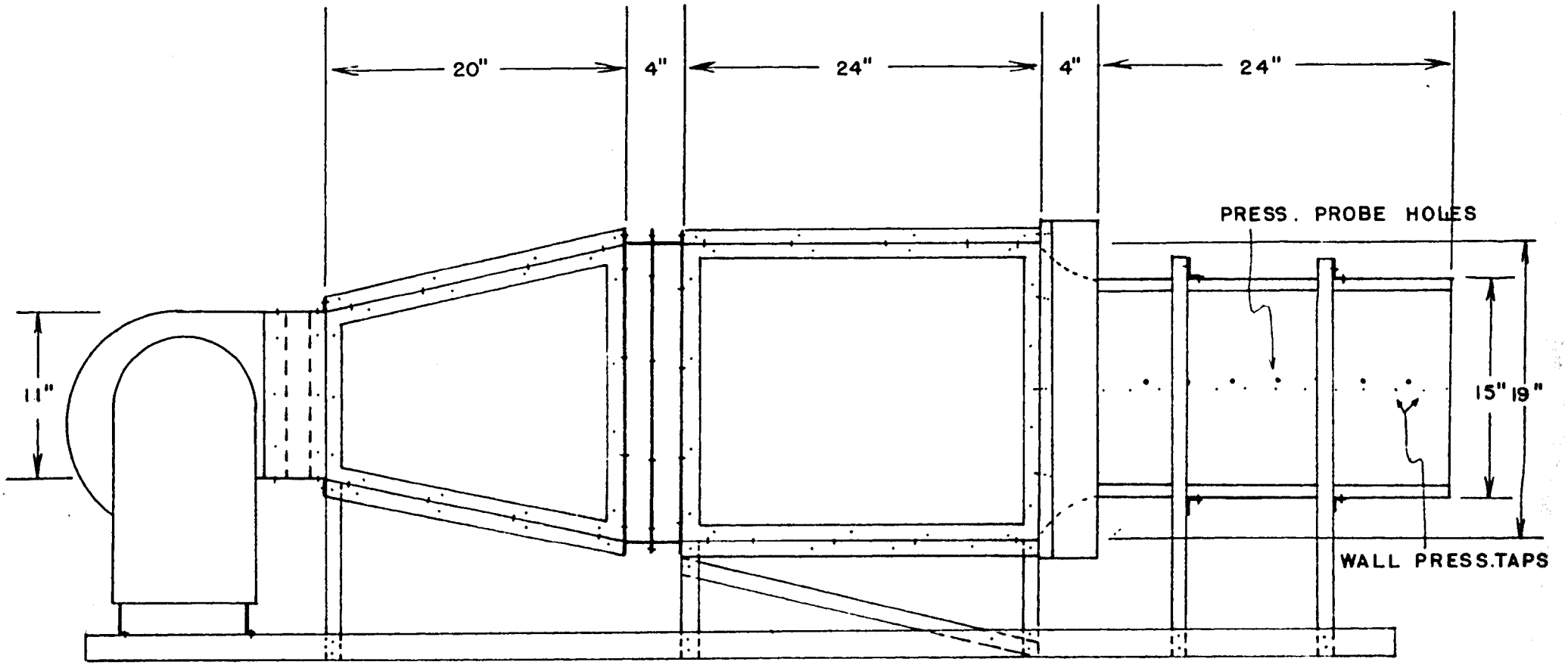

APPARATUS

FIGURE NO. 5

The average between the initial and final pressure was labeled P_o, the reference pressure used to render the equations dimensionless. The maximum variation of P_o during one complete run was 0.5 mm of alcohol or about 0.4 percent of the total pressure.

The first flow patterns analyzed were those of symmetric wall spacings, starting at B = b and increasing by increments of 1/2 = b until the eddy pockets became too long to be contained within the wing walls. The asymmetric wall spacing patterns were run in a similar manner. The extent of each eddy pocket was determined by inserting a thread glued to the end of a thin rod into the flow and observing its behavior.

Next, the wing walls were lengthened by 24b to see what effect this had on the flow patterns, especially the ones that were neutrally stable. Pressure readings in the horizontal plane at vertical quarter points in the expanded section were taken. The resulting total momentum flux and velocity distributions were determined as previously. These were compared with distributions on the plane of symmetry at the same cross-sections and the deviation from two-dimensionality of the particular flow pattern was ascertained. This procedure in effect was a simplified three-dimensional analysis.

4.3 Evaluation of Data

To carry out the study, approximate velocity profiles and flow patterns along with conservation-of-momentum and energy-dissipation relationships are incorporated. These relations make use of both ambient and stagnation pressures measured throughout the flow. For increased refinement in the analysis the turbulence measurements and effects would have to be included.

For all the stable expansions the data were evaluated as follows: First, the pressure distributions were determined. From these the velocity distributions were computed. The flow per unit height at any cross-section was found by taking the area under the curve in the plot of mean velocity versus transverse position. An average flow rate was determined by analyzing flow at each station for a complete run.

Second, the velocity profiles were adjusted to satisfy the condition of constant flow rate on a two-dimensional basis. Then the pressure distributions were modified to satisfy the adjusted velocity profiles.

To construct a flow diagram the centerline of each of the eight stream tubes was located by dividing the adjusted velocity profiles into eight segments of equal area and finding the centroid of each segment. The

flow diagrams were then completed by locating the boundaries of the stream tubes in the xy plane.

The approximate locations of the mean eddy pockets were found by the analysis of these flow diagrams and through the use of thread and rod. These findings were plotted as dotted lines on Figures 17-24.

Through a considered review of the completed flow diagrams, a qualitative determination of the velocity pattern in the eddy pockets was made. This was done to show that there was a velocity distribution throughout the entire expansion, although it did not show up in the measurements. This can be seen more clearly by examining the data sheet and pressure diagrams (Fig. 9 and 10, respectively). The results of this analysis are shown by the dotted lines in Figure 12.

The momentum flux per unit height at each x/b station was calculated using the previously derived expressions, Eq. (8) and (9). In other words, the area under the ambient-pressure curve was subtracted from twice the area under the stagnation-pressure curve. This gave the desired momentum-flux quantities to use as a check on the previously determined velocity distributions.

The determination of the total flow and momentum flux rates from the three-dimensional data was carried

out approximately the same as the previous analysis, the only difference being that a graph showing the vertical distribution of flow and momentum flux was constructed from the results of the vertical quarter-point analysis.

The flow and the momentum flux at each of the quarter-points was calculated as previously with the results plotted on a graph of flow rate versus vertical distance and momentum flux versus vertical distance (see Fig. 16). The total quantities were determined by graphical integration of Eq. (9), as pertaining to the vertical flow and momentum-flux distribution diagrams, Figure 16.

The measured value of the two-dimensional flow rate should remain unchanged or increased slightly from section to section due to boundary layer effects. This increase should be present in both the two and three-dimensional methods of analysis. Again for both cases the momentum flux from section to section should remain constant or decrease slightly due to the previously mentioned neglected Reynolds factors.

To find the loss coefficient C_L an energy distribution diagram was constructed by multiplying, point by point, the total pressure by the velocity and plotting the product versus the transverse distance, y. The

energy flux at each successive section was determined by a graphical integration of Eq. (12) by measuring the area under the previously constructed energy-distribution diagrams. By plotting the energy flux at each successive section versus the axial location of the section and connecting them with a smooth curve, the loss coefficient, C_L, of Eq. (12), was analytically determined.

4.4 Experimental Results

It should be noted here that the flow and momentum flux rates should not vary but the results of the analysis indicate they do. This discrepancy would indicate that the collected data were inaccurate or inadequate. It should be further pointed out that the apparent accuracy of the results depend upon whether a two or three-dimensional method of analysis was used. All of this will clearly be understood in the following paragraphs. The poor results shown by the two-dimensional analysis led to the simplified three-dimensional analysis and a check on the original data.

For the ease of explanation and discussion the experimental runs were divided into two groups, the first containing stable-equilibrium flow conditions and the second containing neutral-equilibrium flow conditions.

In the stable runs, B = b, B = 1 1/2b, B = 2b, both the continuity and momentum relationships were satisfied as shown in Figures 6 and 7. There was a noticeable increase in measured momentum and flow rates in the B = 2b run, but the flow was still stable. These increases amounted to about 20 percent in each case. The two-dimensionality was reasonably well satisfied for the smallest two spacing ratios of the three. But for the larger one, there were separation pockets in evidence on the floor and roof of the expansion causing a concentration of flow along the horizontal plane of symmetry. The concentration of flow rendered the two-dimensional analysis inaccurate and accounted for the large increase in flow and momentum flux rates. All the asymmetric-wall-position runs were stable, but as shown in Figure 6, only a = o c = b satisfied the continuity and momentum relationships. In all other spacings these quantities increased markedly. Again there were separation pockets on the floor and roof of the expansion producing a condition where two-dimensionality did not exist.

For the remaining spacings studied two-dimensionally, B = 2 1/2b, B = 3b, B = 4b, the flow existed in a state of neutral equilibrium. The analysis of the gathered data showed large increases in momentum flux and flow rate as shown in Figure 7. In some cases,

the increase amounted to more than 50 percent. But for all the spacing ratios greater than B = 2b there were separation pockets on the floor and roof of the expansion. These separation pockets seemed to account for the systematic error that occurred in the two-dimensional analysis. This error points out the need for a three-dimensional analysis in a 10 x 1 slot.

Analysis of the data taken from the three-dimensional method showed that the flow rate and momentum flux remained essentially constant from station to station when total flow was considered. The measured momentum flux increased 6.8 percent from x/b = o to x/b = 32 and the measured flow rate increased 5.3 percent as shown in Figure 7. The boundary effect which was not previously considered could have caused the 6.8 and 5.3 percent increases.

The energy-loss coefficients for the stable runs, for both symmetric and asymmetric spacings, were much less than for the neutrally stable runs. Figure 9 depicts the stable-flow energy losses while Figure 8 shows the neutrally stable. The loss coefficient seemed to have a direct relation to the number and size of the eddy pockets. The loss coefficient for the stable symmetric runs was 0.26, while for neutrally stable symmetric runs it was 0.55. The asymmetric-run loss coefficient for all

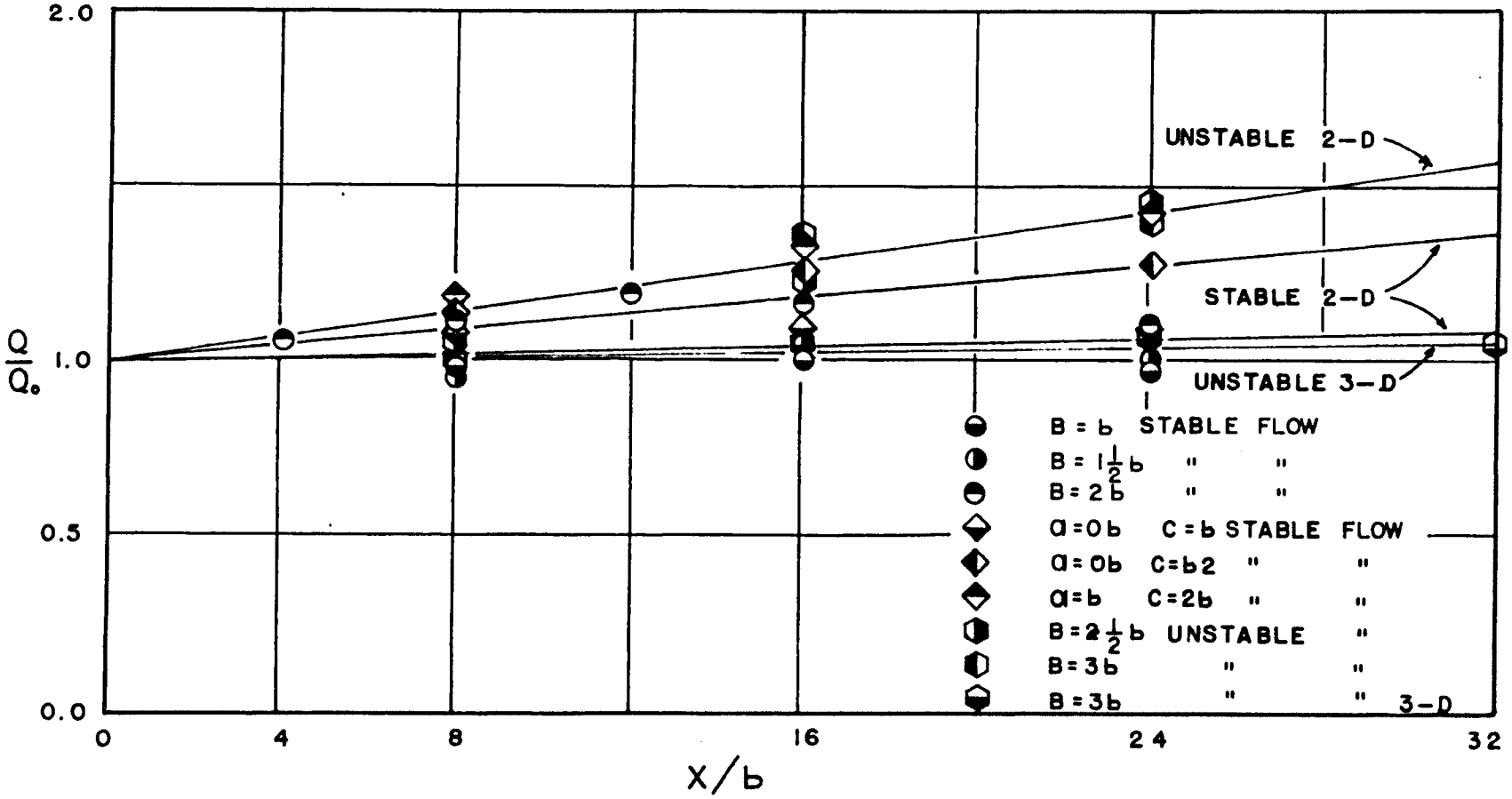

CONTINUITY QUANTITIES

FIGURE NO. 6

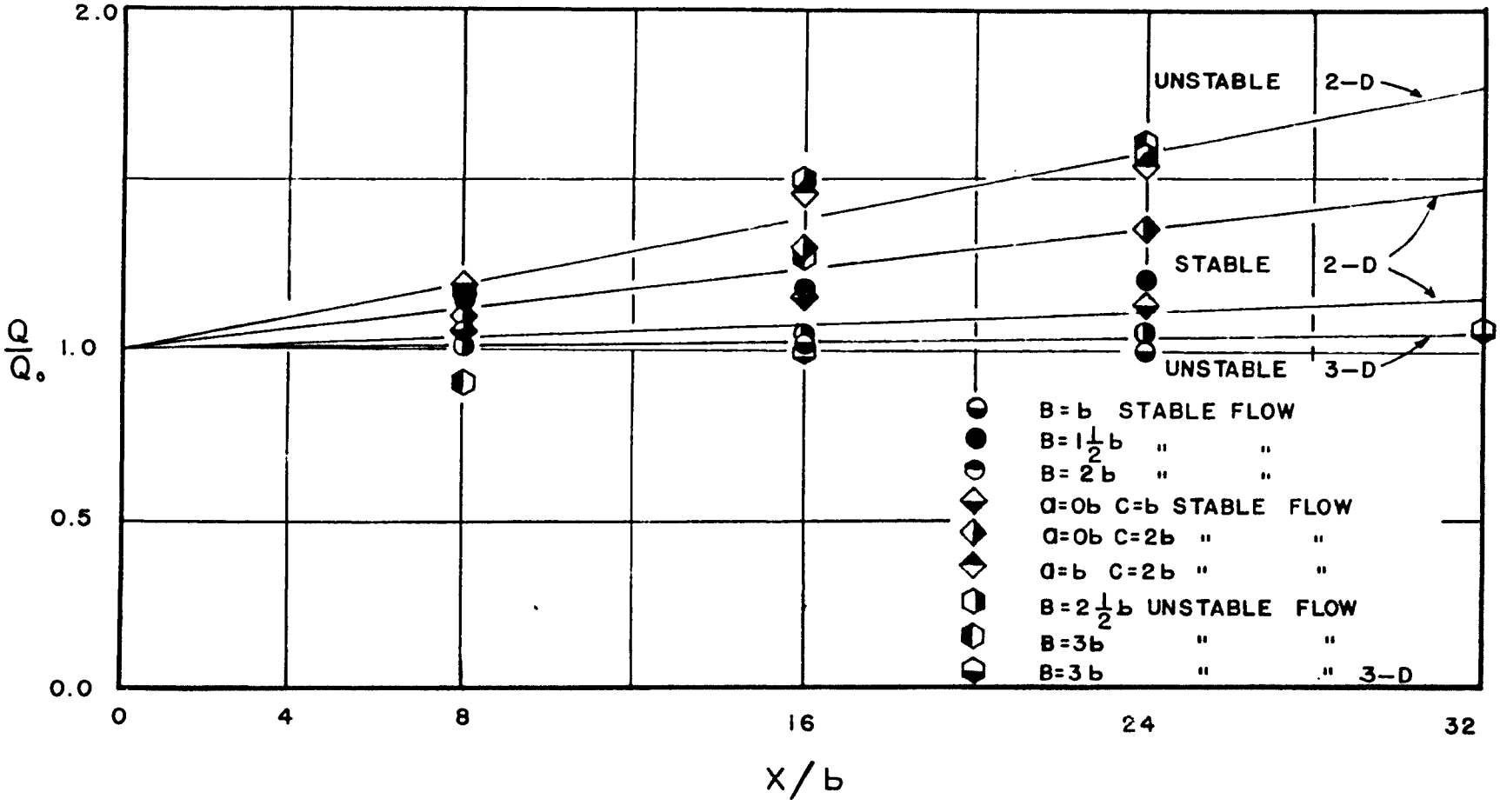

MOMENTUM QUANTITIES

FIGURE NO. 7

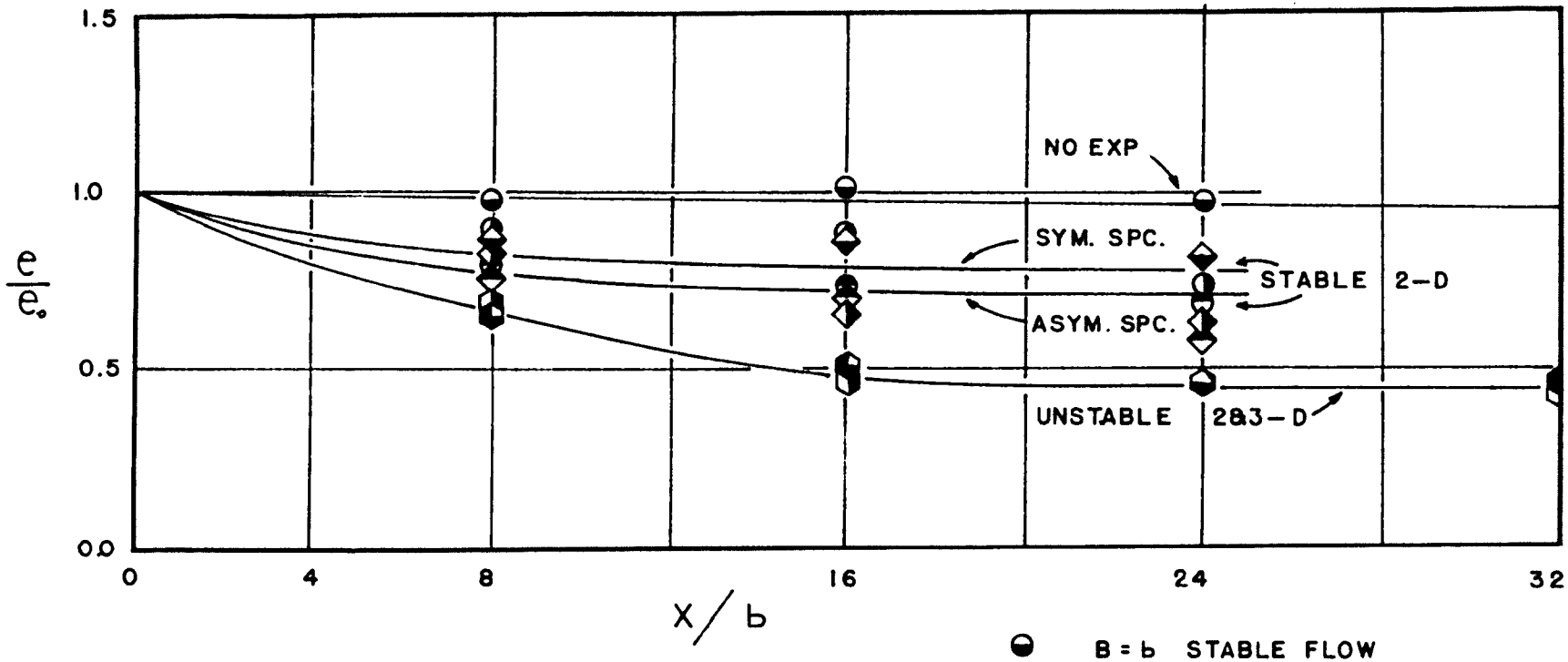

B = b STABLE FLOW
B = ½b " "
B = 2b " "
a = 0b c = b STABLE FLOW
a = 0b c = 2b " "
a = b c = 2b " "
B = 2½b UNSTABLE FLOW
B = 3b " " 2-D
B = 3b " " 3-D

ENERGY DISSIPATION RATES

FIGURE NO. 8

expansion ratios was 0.32. For the run of B = b, or no expansion, the loss coefficient due to viscous action alone was quite small, 0.035. On the spacing B = 3b the loss coefficient was determined using the corrected results of the three-dimensional analysis plus using the two-dimensional analysis data. The two sets of data gave exactly the same results. See Figure 8.

The existence of two very large eddy or separation pockets was discovered while running an exploratory vertical ambient-pressure traverse. These pockets were located on the floor and roof of the expansion (see Fig. 26). Their magnitude and location were further determined through use of the rod and thread.

4.5 Interpretation of Results

When the flow was in stable equilibrium with symmetrical wall spacings, the runs showed that the flow behaved two-dimensionally as expected with the mean streamline pattern symmetrical about the centerline. These conditions proved the validity of the two-dimensional method of analysis for certain spacing ratios. The increases in momentum-flux and flow rate for the B = 2b spacing ratio, with stable flow, might have been due to experimental error but more likely can be attributed to the flow approaching neutral equilibrium and an invalid

two-dimensional analysis caused by the existence of the separation pockets. The asymmetric-spacing ratios produced stable flow, but showed an increase in momentum-flux and flow rate. These increases probably resulted from spacing ratios that do not lend themselves to a two-dimensional method of analysis.

All the large quantity increases shown for the remaining symmetric spacings studied, B = 2 1/2b, B = 3b, B = 4b, could have stemmed from errors in measurement or again an invalid method of analysis. For this reason a simple three-dimensional method of analysis was run to check if the total momentum-flux and total flow-rate quantities still showed increases. The small systematic increases in the measured values of these known constant quantities that did occur were consistent with secondary effects of boundary-layer growth along the bottom and top of the test section.

The separation pockets and the eddy pockets which were more evident at some spacing ratios than others were in effect large energy dissipators. In this respect they had a direct effect on the loss coefficients. The size and location of the pockets thus had a controlling effect on the values of the loss coefficients. The separation pockets on the top and bottom of the expansion caused a

concentration of flow about the horizontal centerline. This concentration was of such magnitude that the flow may have been forced into a virtual contraction before expanding.

CHAPTER 5

CONCLUSIONS AND RECOMMENDATIONS

5.1 Conclusions

There were two very interesting phenomena shown by this experiment: the instability of the flow at certain expansion ratios and the invalidity of the two-dimensional method of analysis for these cases.

The limiting expansion ratio for neutral equilibrium occurred somewhere between B = 2b and B = 2 1/2b. With this degree of expansion the resulting two eddy pockets became large enough and the over-all ambient-pressure difference was large enough so that it could conceivably affect the flow pattern due to the forces created by the pressure difference. This difference existed not just throughout the eddy pocket but also along the walls as shown by the wall pressure readings. This finding is supported in a paper by H. R. Muller[4] where he shows that by changing the pressures along the boundaries and in the eddy pockets caused by a jet, the jet can be sucked from one wall to the other.

The flow followed one pattern as long as there was nothing in the flow to disturb it, but as soon as a

deflection device was inserted in the flow which changed the pressure distribution, it assumed and retained a different flow pattern. If this instability were predictable, the engineer could more effectively design aerodynamic and hydraulic structures wherein sudden expansions occur.

The more interesting of the two phenomena and the one less expected at the initiation of the research was the invalidity of the two-dimensional method of analysis for certain expansion ratios. This fact was not appreciated in the author's original considerations of the investigation, but may well be the most significant information determined from it. The invalid two-dimensional method of analysis could be caused by several things. First, the wind tunnel used was not a true two-dimensional tunnel although it was designed to give a good approximation to two-dimensional flow. However, the continuity and momentum relationships were satisfied reasonably well for some cases. Also, when the wing walls were removed, the flow behaved as nearly as could be determined like a two-dimensional submerged jet.[5] These factors clearly point out that the tunnel design was satisfactory and that the answer lies elsewhere. Secondly, to obtain an increase in flow rate and momentum as shown by the two-dimensional analysis there must have been a concentration

of flow along the horizontal plane of symmetry. The probable cause of the flow increase was an actual forcing of the flow toward the center by separation pockets on the floor and roof of the expansion as shown by Figure 25. (Eddy pockets refer to vertical quasi-stable eddies resulting from separation because of the geometric boundary expansions, while separation pockets refer to horizontal quasi-stable eddies along the floor and roof of the expansion due to separation resulting from the adverse pressure gradient.) These separation pockets, not foreseen in the original consideration of the experiment, in the author's opinion, caused the large concentration of flow along the horizontal centerline. This situation led to the large increases in flow rate and momentum quantities from section to section; therefore, it was considered the major reason for the invalidity of the two-dimensional method of analysis.

These separation pockets form because of the adverse pressure gradient in the finite flow field. The flow leaves the jet at a high velocity and low ambient pressure, then enters the expansion where there is a deceleration and an increase in pressure. These facts, plus boundary-layer growth producing further deceleration on flow near the boundary, all add together to induce a condition favorable to separation.

At the larger expansion ratios, B = 2 1/2b and up, the separation pockets along with eddy pockets caused a condition in which the flow behaved as though it passed through a mechanical contraction. This condition only existed from the tunnel exit to approximately x/b = 2 downstream, at which section the flow commenced expanding.

In a contraction the velocity increases, producing a corresponding decrease in ambient pressure, while in an expansion the opposite is true. If one examines a plot of ambient pressure along the centerline for symmetric expansions as shown by Figure 11, it will become quite evident that for this study the pressure decreases before it increases, indicating there is a contraction and then an expansion. This further verifies the belief that there was a concentration of flow at the centerline causing the two-dimensional method of analysis to be invalid.

The variation of loss coefficient from 0.26 for conditions of symmetric-stable-equilibrium flow, to 0.32 for asymmetric-stable flow, to 0.55 for symmetric-neutral-equilibrium flow, can be related directly to the size, location and number of eddy and separation pockets or more accurately to the area of the high turbulence generating regions. The energy loss may also be effected by the amount of contraction due to the separation and eddy pockets. This contraction effect, which would produce

an increase in velocity leading to a greater loss in the expansion that followed, plus the energy loss of the contraction itself could be related to the loss coefficient. But, because of the small magnitude of the contraction effect as pointed out by Figure 11, it was felt that the differences in area of the turbulence-generating zones for different spacing ratios was the main cause for the different values obtained for the loss coefficient.

The concept of the variance of loss coefficient with the variance in the area of the turbulence generation zones was supported by the fact that the number and size of the eddy and separation pockets increased as the flow pattern, produced by the wall conditions, went from stable-equilibrium to neutral-equilibrium.

For the stable symmetric runs there were only two relatively small eddy pockets which are clearly pointed out by the dotted lines in Figures 18 and 19. Therefore, they produced the smallest loss coefficient. There were different combinations of the number and size of pockets for the runs of asymmetric spacing (see Figs. 22-24). But each of these combinations would provide more energy dissipation than did the conditions for the stable symmetric runs. This corresponds with the fact that these conditions produced an intermediate loss coefficient.

For the neutral-equilibrium flow conditions there were two eddy and two separation pockets. At each spacing the size of the four pockets were measurably larger than the comparable ones for all the other flow conditions (see Figs. 20 and 21). This very clearly indicates the reason why the neutral-equilibrium flow condition generated the largest loss coefficient.

From further study of the energy dissipation it was noted that the loss coefficients for all the neutral-equilibrium runs were approximately 0.55. This pointed out that the loss coefficient was independent of wall spacing. It was also shown that two-dimensional-analysis data gave the same loss coefficient as the three-dimensional-analysis data. This demonstrated that a two-dimensional method of analysis could be used to approximate losses in an expansion even if the flow pattern is not two-dimensional. This conclusion arose from a close examination of the discharge portion of Figure 26 which showed that for large expansions the vertical gradients of mean velocity were slight. Thus, when the evaluation of energy loss was determined by Eq. (12), the velocity term for both the two and three-dimensional methods of analysis were approximately equal producing similar loss coefficients.

The original hypothesis that the role turbulence plays is quite small, and, therefore, can be neglected was confirmed upon examination of the loss coefficient for no expansion.

5.2 Recommendations

The author feels that in any further study of this kind several things should be done.

1. The unstable wall positions should be located precisely and pressures checked for both maximum and minimum spacing.

2. The instability should be studied with a three-dimensional method of analysis.

3. If possible, a turbulence analysis should be run and the losses calculated.

4. A smaller width-to-height ratio of the vertical exit slot should be checked two-dimensionally.

5. A more intensive program of obtaining pressure distributions throughout the eddy pockets should be undertaken.

6. A more detailed study of the size, location, and pressure distributions in the separation pockets on the floor and roof should be carried out.

APPENDIX

The turbulence was neglected for the following reasons: Upon analyzing expansion experiments run by others[8] where turbulence was considered, it was decided that for this study it could be neglected; and also it was felt that it was beyond the scope of the research. The viscous stresses were neglected because, as is shown in an experiment by J. Laufer on the structure of turbulence, they were very small, having little over-all effect.[9] The body forces were neglected because air was measured in air. The vertical and transverse velocity components w and v were not considered because it was felt that the measurement of them was again beyond the scope of the research.

Only one representative series of data, plus the corresponding pressure and velocity diagrams, was included. See Figures 9 through 16. The pressure and velocity diagrams of all other runs were identical in structure. The series included was an unstable one, B = 3b, which showed that when the main body of the flow was along the right side of the expansion, the pressures were practically a mirror image of the pressures when the

flow was along the left side. The velocity diagrams shown are with the flow along the left side.

Because of the invalid two-dimensional method of analysis, the continuity relationship was not strictly followed in drawing the corrected velocity diagrams in the unstable cases. The diagrams were constructed by averaging the three-dimensional analysis results and using this curve as the correct continuity curve. The corrected velocity diagrams shown have the uncorrected points along with the "correct" velocity distribution.

All of the mean streamline diagrams, Figures 17 through 24, are self-explanatory. The only ones presented here are those that show basic patterns.

The unstable-condition diagrams included here, B = 2 1/2b and B = 3b, include data from flow along one wall only. The similarity between the two flow patterns, right and left, for any one expansion ratio is so close that only one diagram is needed to demonstrate the flow pattern characteristics.

DATE: 7-22-65 TIME: 12:45 PM

TEMP: Start 27° C Finish 28.5° C

P_o: Start 123 mm Finish 123 mm

WALL WIDTH: B 2 1/4" - 3b ECCENTRICITY: 0

MANOMETER SLOPE: 2:1 UNITS: mm

Wall Press. (Amb. pr.)

Flow	Right	
-88	-71	0
-43	-71	6
-43	-46	12
-20	-17	18
- 9	- 8	24
Flow	Left	
-70	-90	0
-71	-50	6
-46	-41	12
-18	-19	18
- 7	- 8	24

REMARKS

L - flow left

R - flow right

Flow was unstable

Total Pressure y 1/4" int.

Ambient Pressure y 1/4" int.

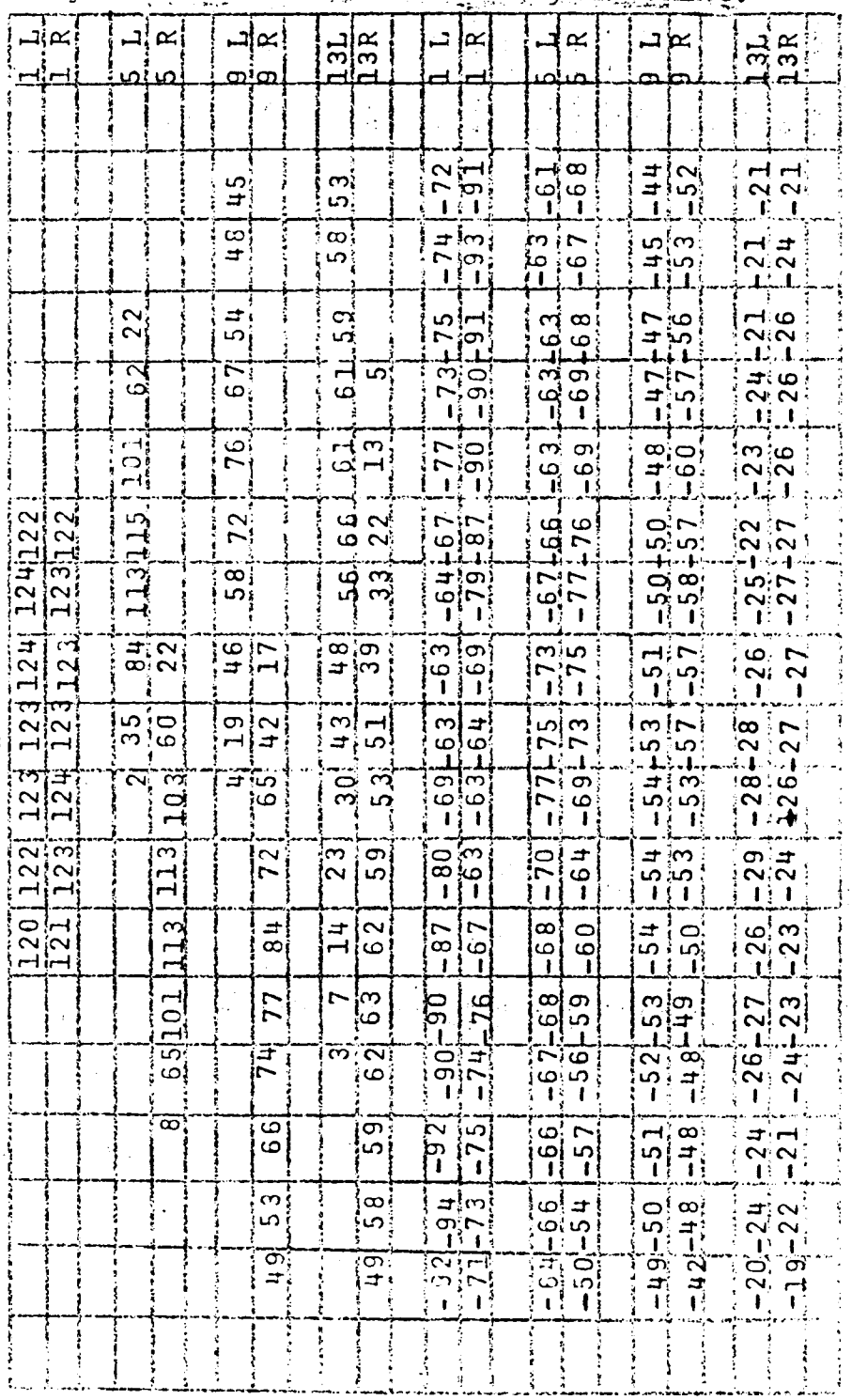

Figure 11.

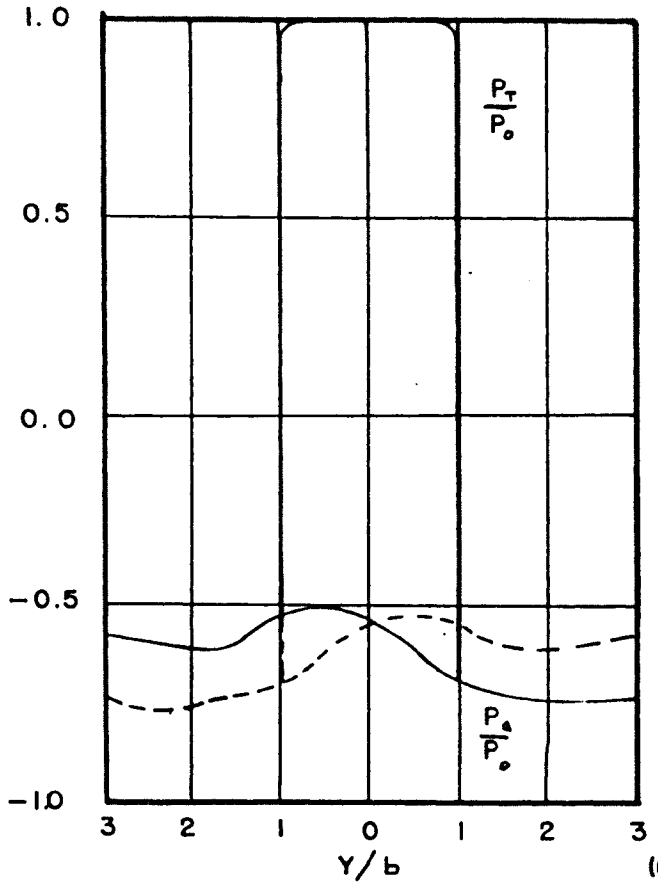

(a) X/b = 0

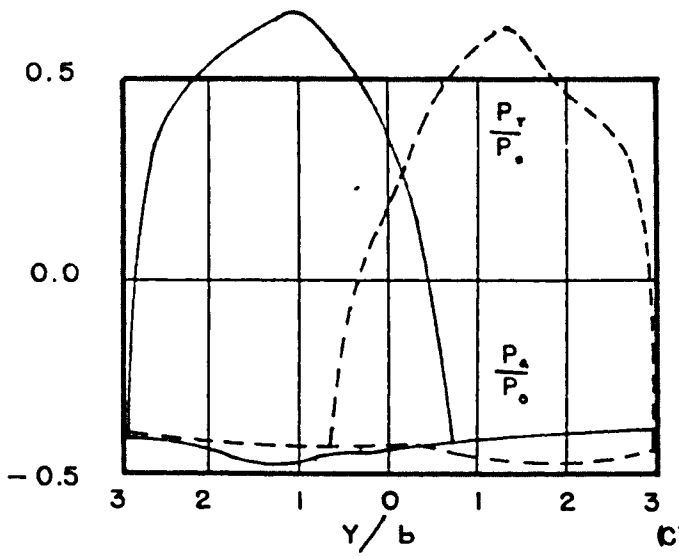

(c) X/b = 16

PRESSURE DISTRIBUTION DIAGRAMS

B = 3b DATA TAKEN 7-22-65

FIGURE NO. 10

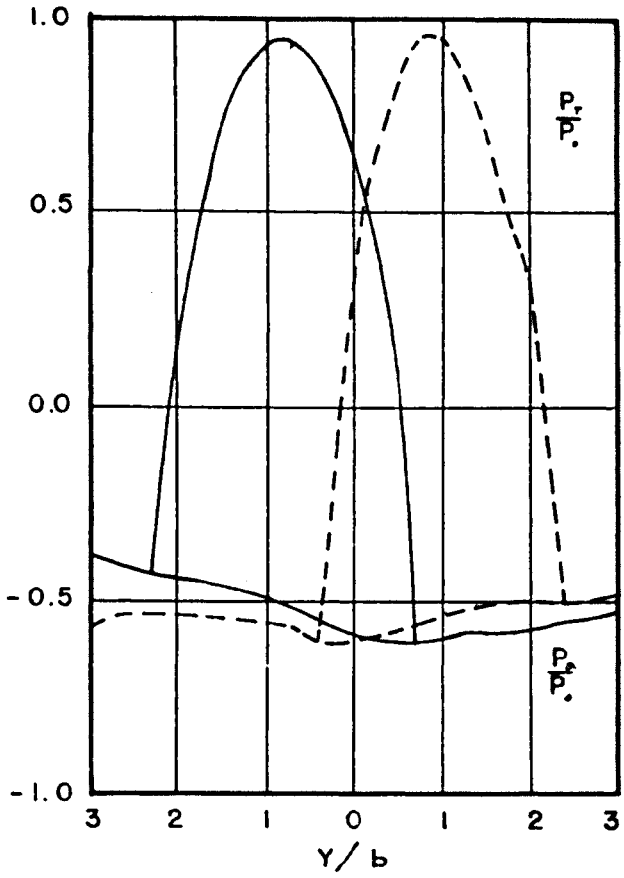

(b) X/b = 8

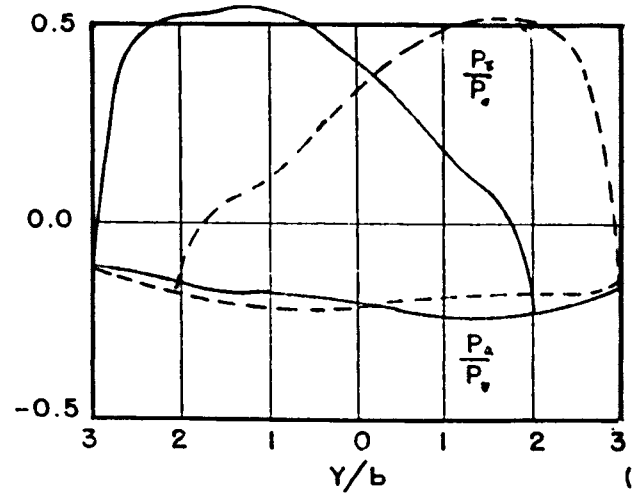

(d) X/b = 24

PRESSURE DISTRIBUTION DIAGRAMS

B=3b DATA TAKEN 7-22-65

FIGURE NO. 10 CONT'D.

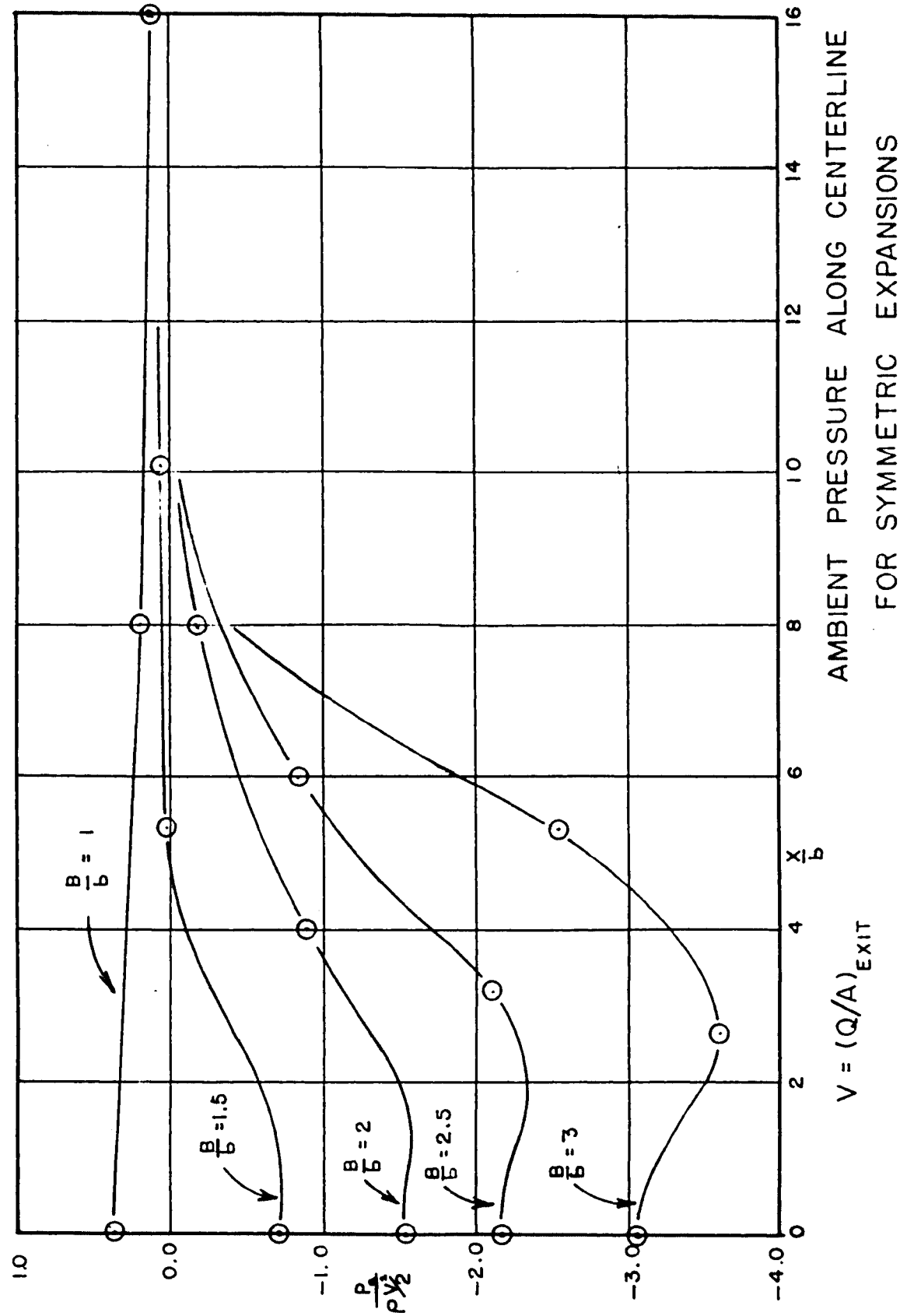
AMBIENT PRESSURE ALONG CENTERLINE
FOR SYMMETRIC EXPANSIONS
V = (Q/A)EXIT
B/b = 1
B/b = 1.5
B/b = 2
B/b = 2.5
B/b = 3
X/b
P/ρV²/2
1.0
0.0
-1.0
-2.0
-3.0
-4.0
0
2
4
6
8
10
12
14
16

FIGURE NO. 11

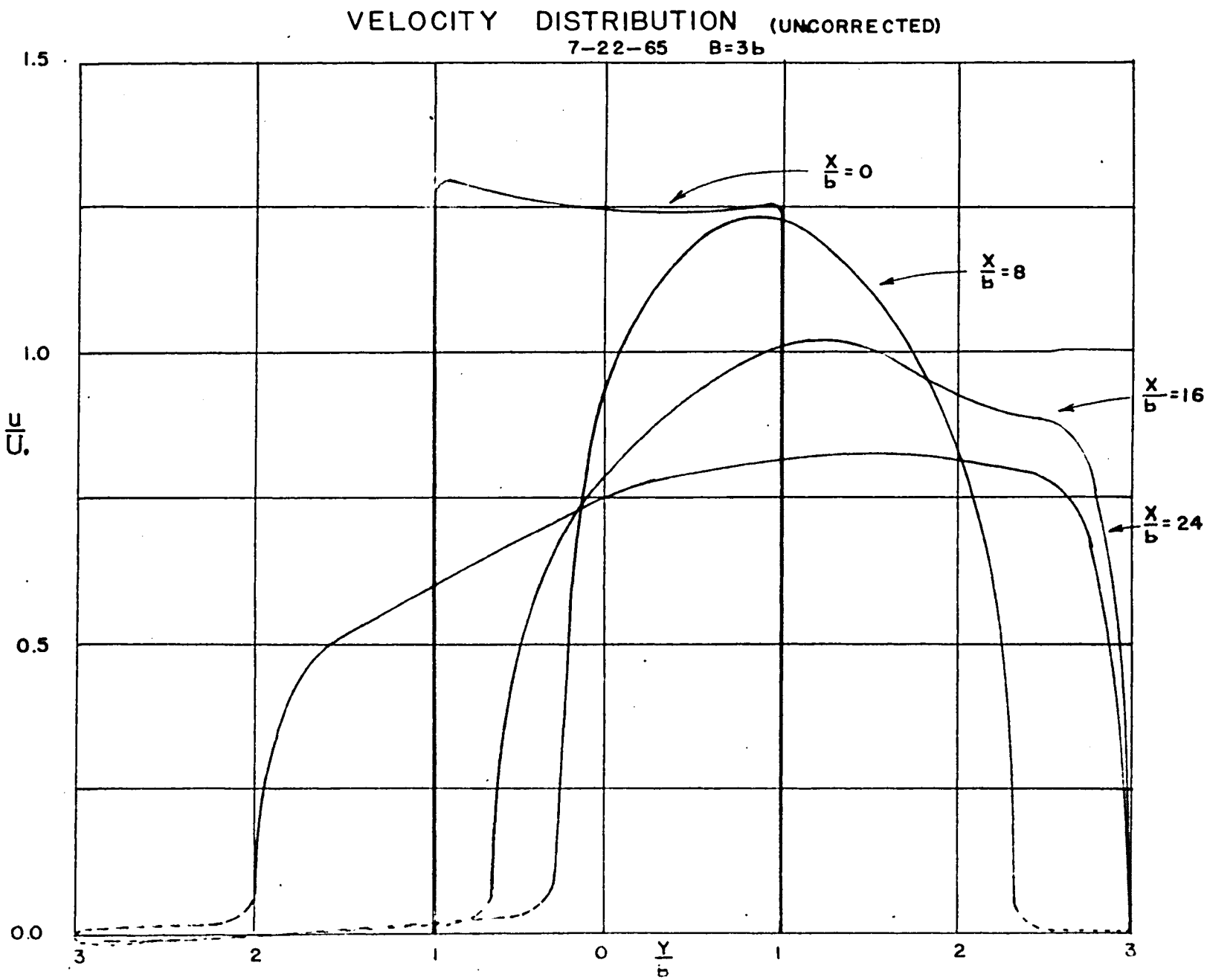
VELOCITY DISTRIBUTION (UNCORRECTED)
7-22-65 B=3b
1.5
1.0
0.5
0.0
U/U.
X/b = 0
X/b = 8
X/b = 16
X/b = 24
3
2
1
0
Y/b
1
2
3

FIGURE NO. 12

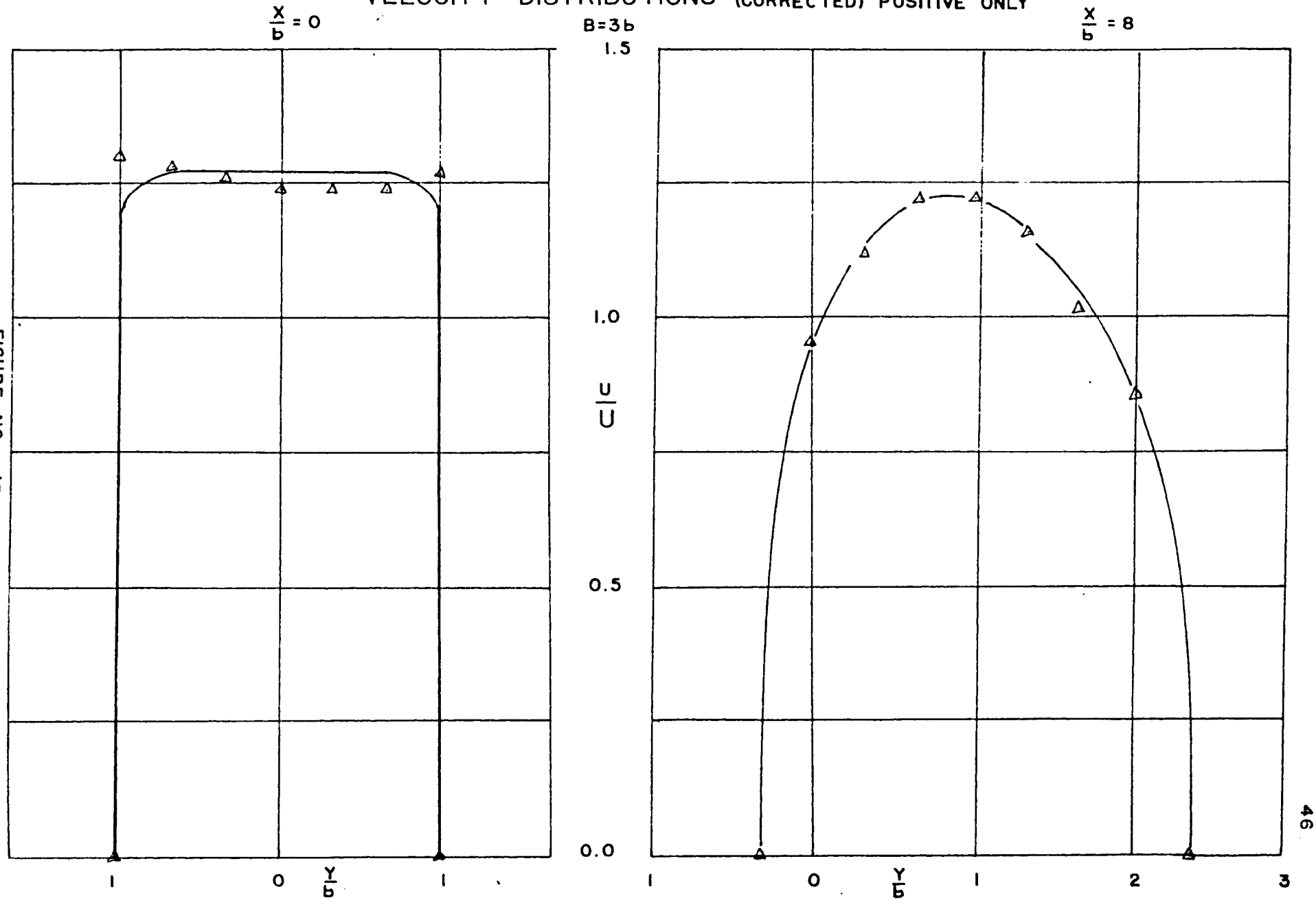
VELOCITY DISTRIBUTIONS (CORRECTED) POSITIVE ONLY
X/b = 0
B=3b
X/b = 8
1.5
1.0
0.5
0.0
U/U
-1
0
Y/b
1
-1
0
Y/b
1
2
3

FIGURE NO. 13

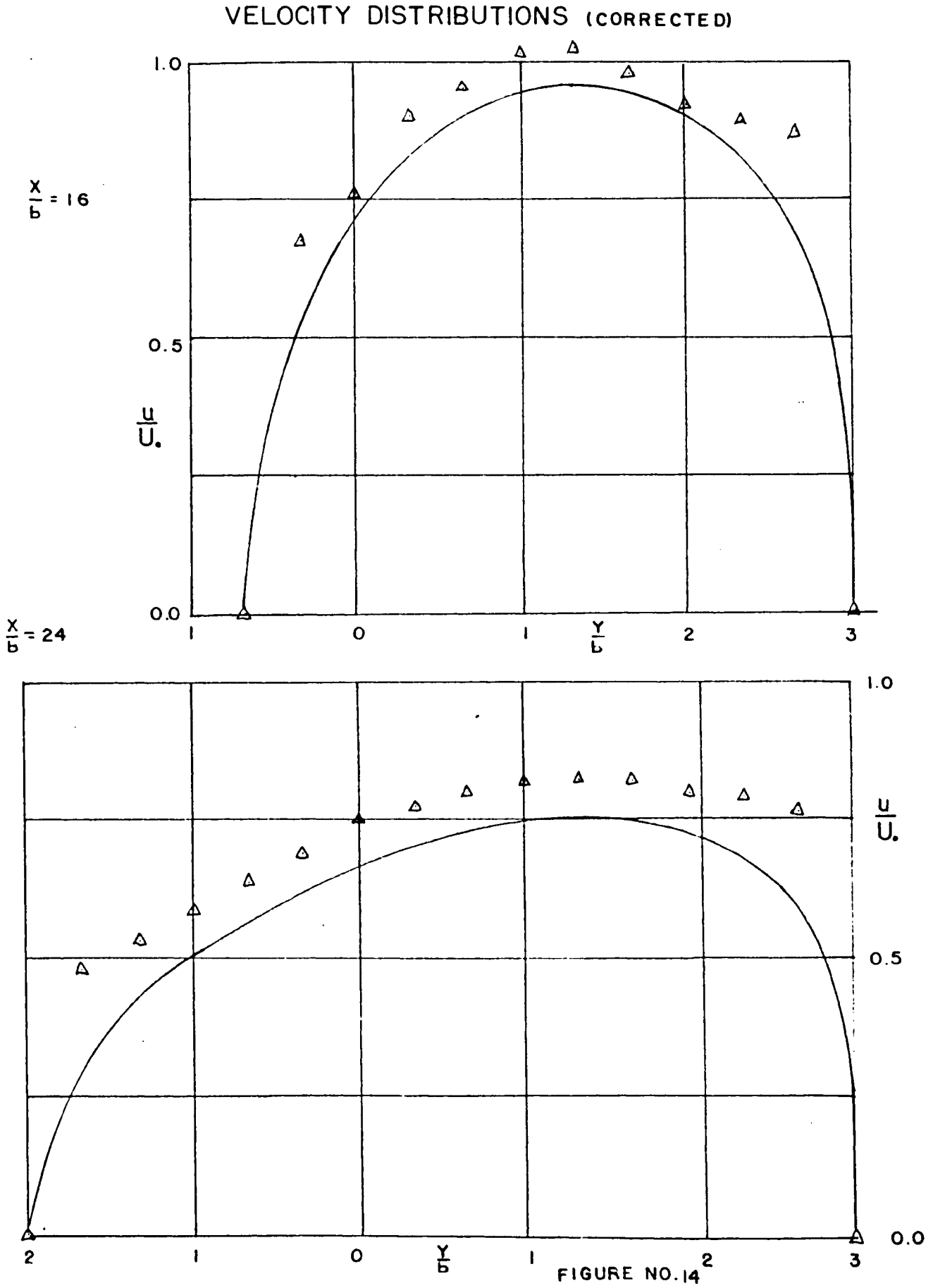
VELOCITY DISTRIBUTIONS (CORRECTED)
X/b = 16
X/b = 24
1.0
0.5
0.0
u/U.
-1
0
1
2
3
Y/b

FIGURE NO. 14

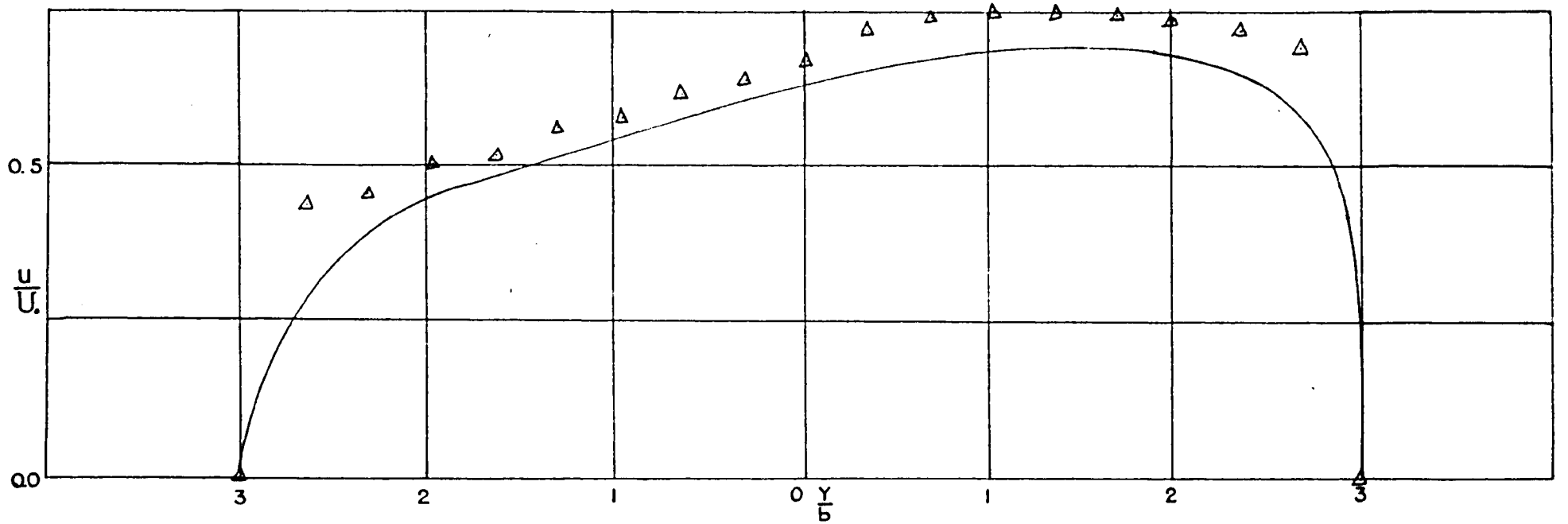

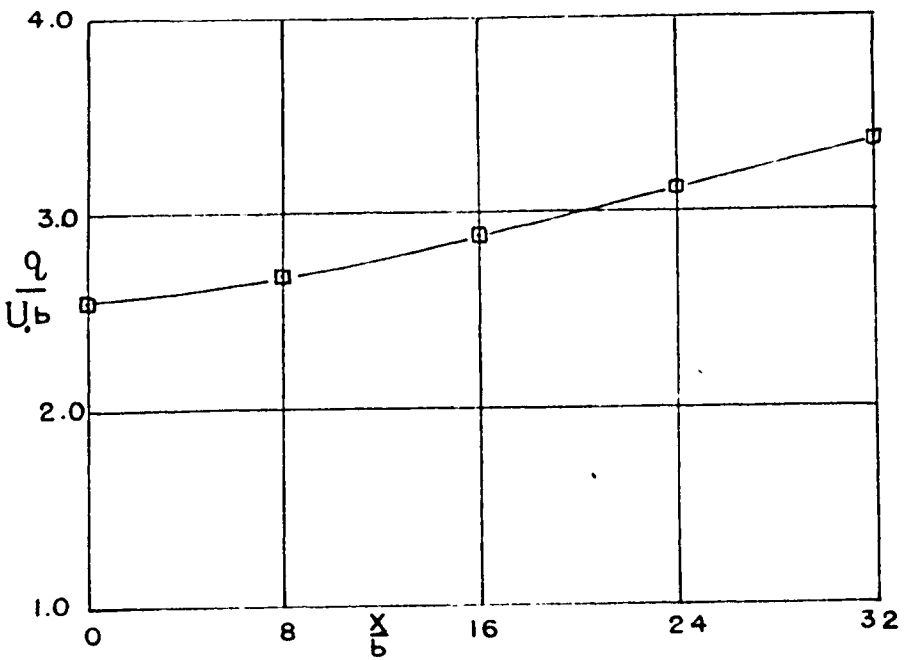

FIGURE NO. 15

(ABOVE)

VELOCITY DISTRIBUTION (CORRECTED)

B=3b $\frac{X}{b}$=32

(LEFT)

CONTINUITY RELATION (CORRECTED)

B = 3b

CONTINUITY & MOMENTUM DISTRIBUTIONS

THREE – DIM. ANA.
UNSTABLE FLOW
SYMMETRIC WALL COND.
B = 3b

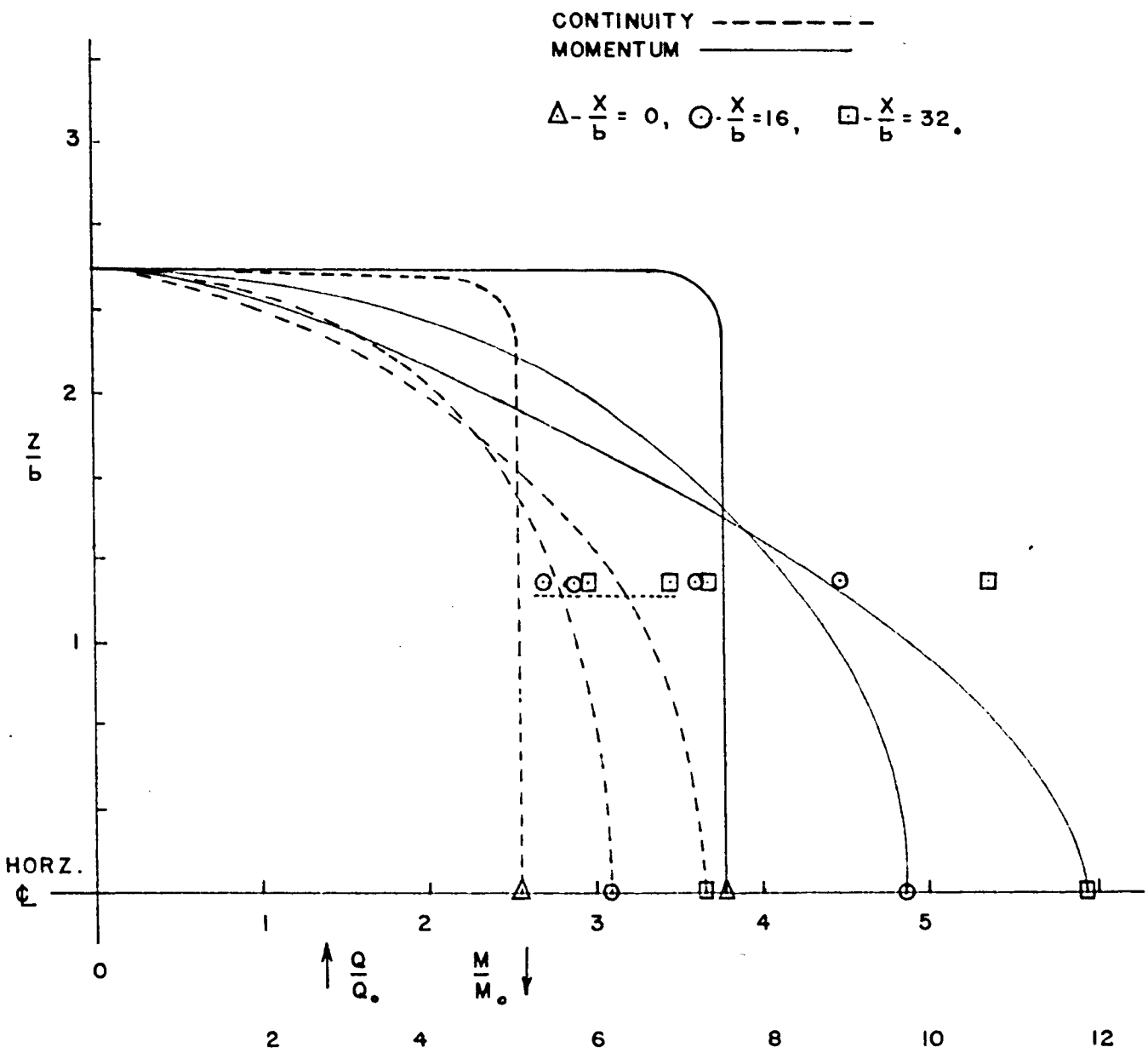

FIGURE NO. 16

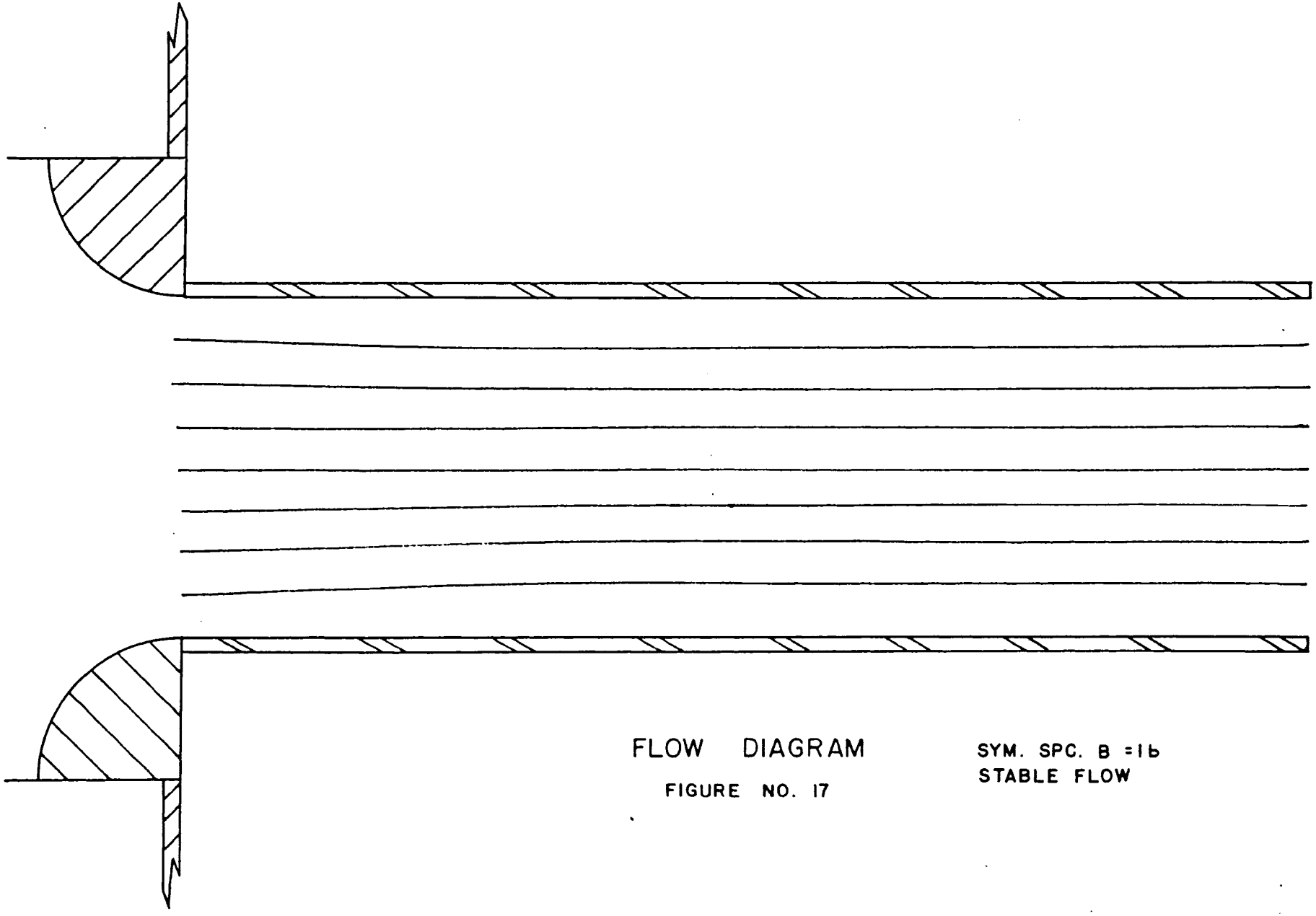

FLOW DIAGRAM

FIGURE NO. 17

SYM. SPC. B = 16
STABLE FLOW

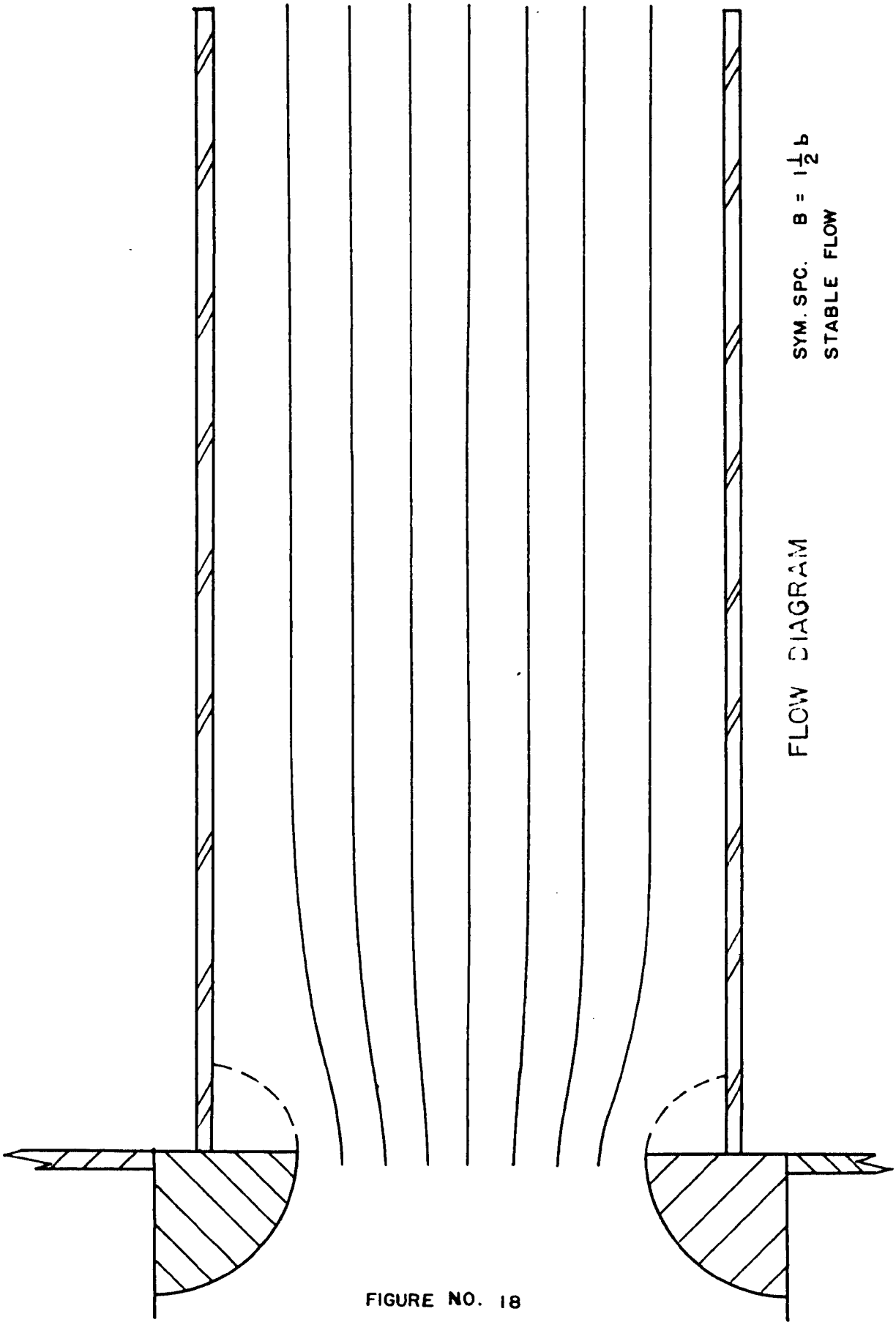

FIGURE NO. 18

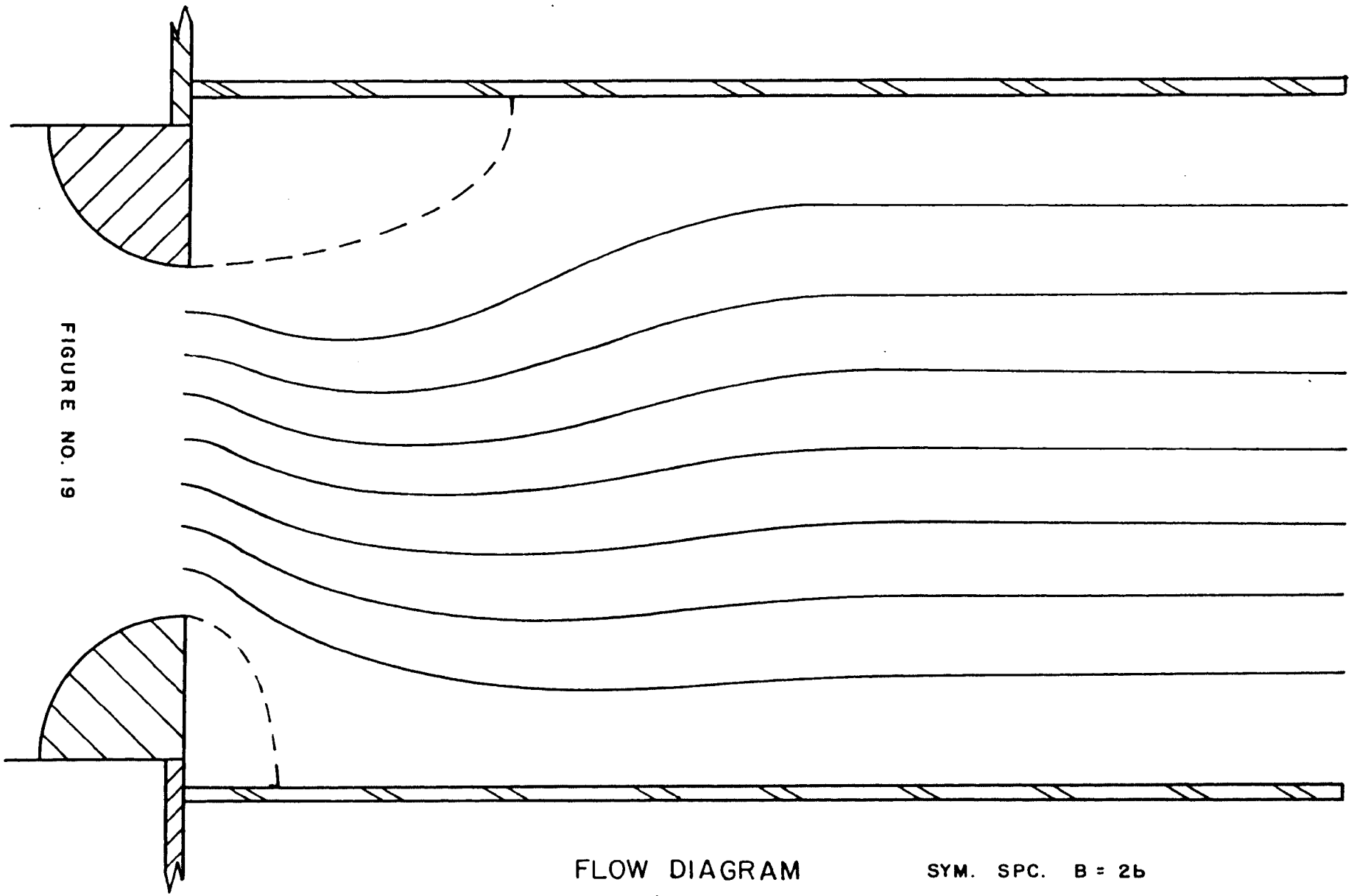

FIGURE NO. 19

FLOW DIAGRAM

SYM. SPC. B = 2b

STABLE FLOW

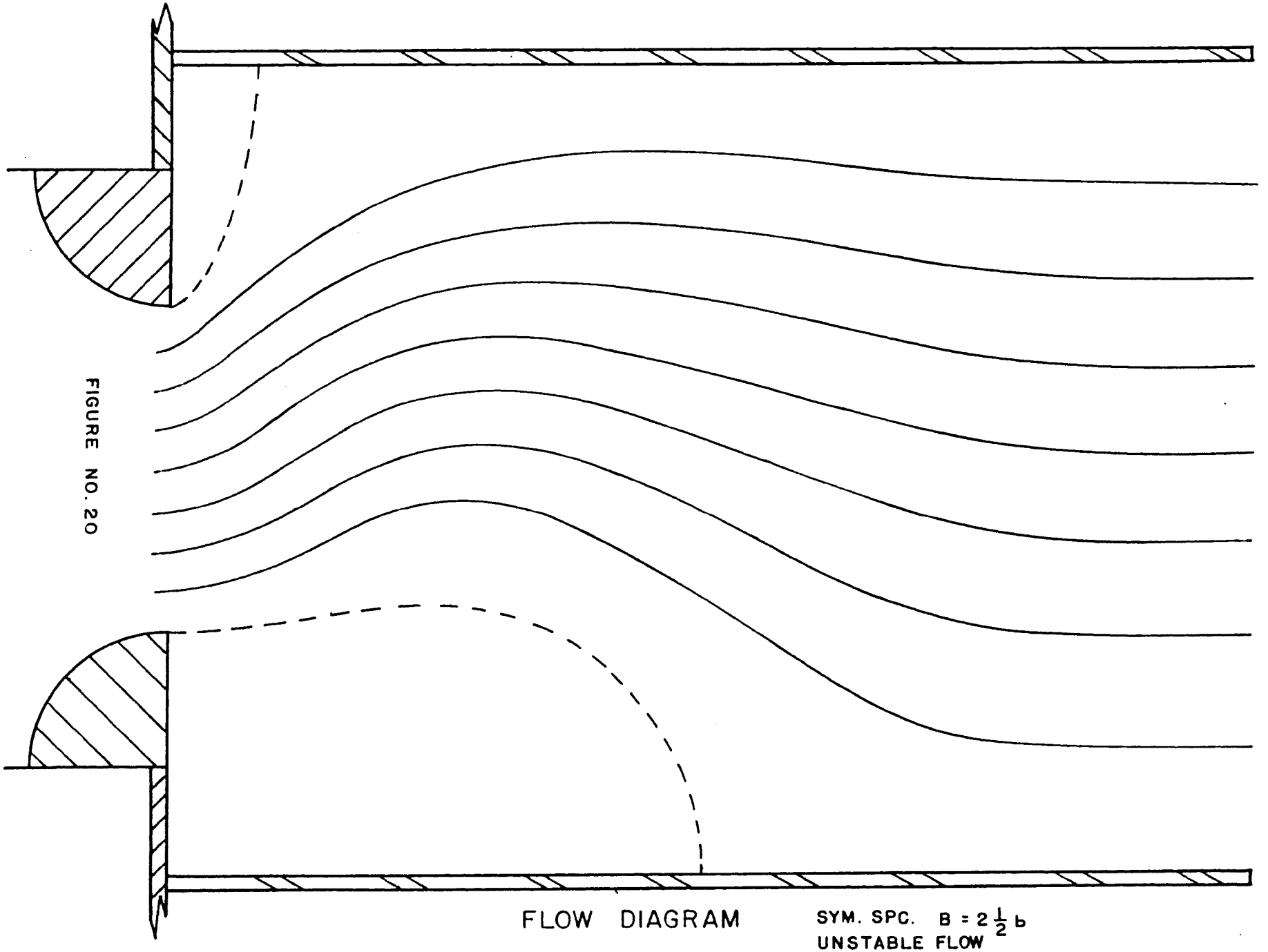

FIGURE NO. 20

FLOW DIAGRAM SYM. SPC. $B = 2\frac{1}{2}b$
UNSTABLE FLOW

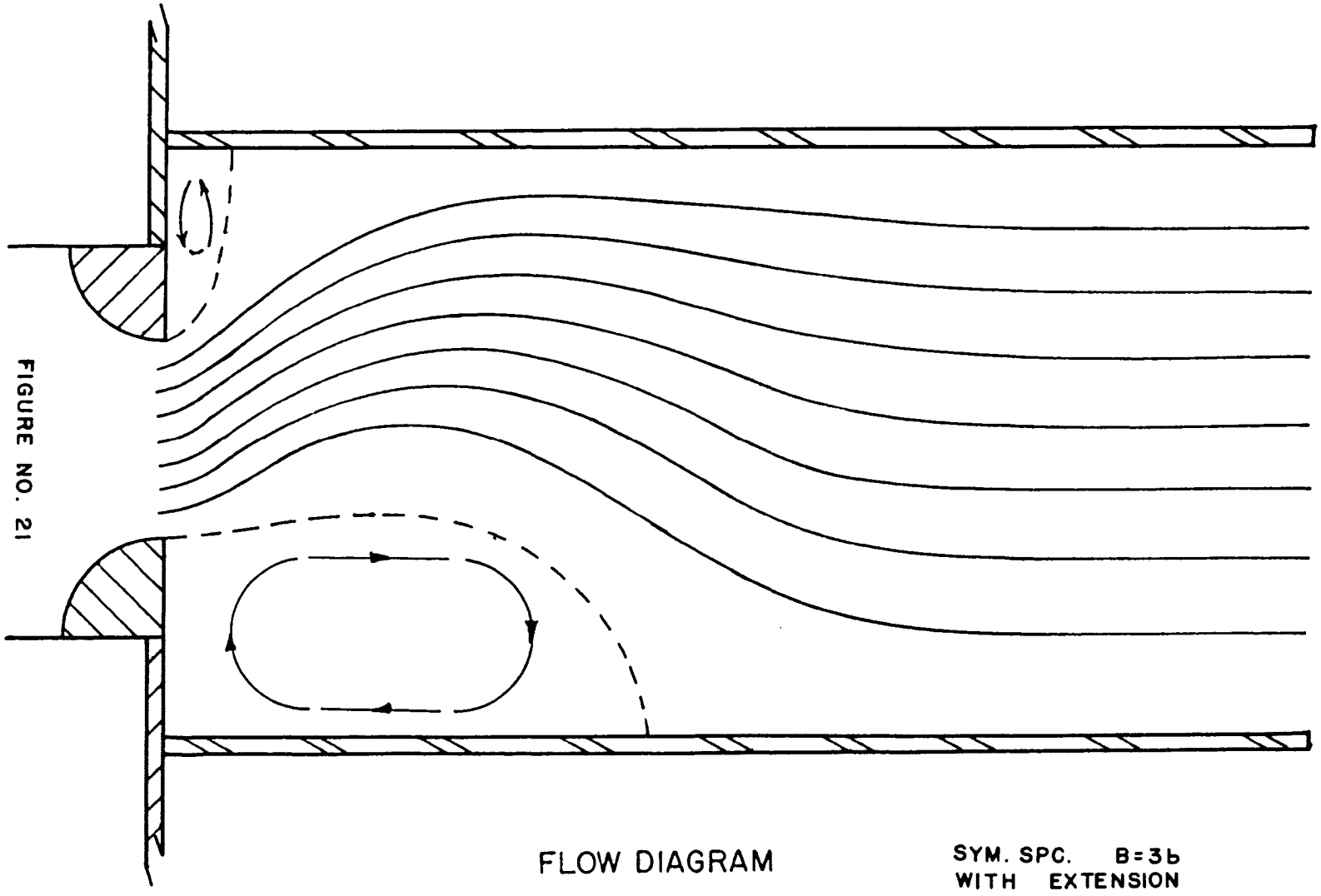

FIGURE NO. 21

FLOW DIAGRAM

SYM. SPC. B=3b
WITH EXTENSION
UNSTABLE FLOW

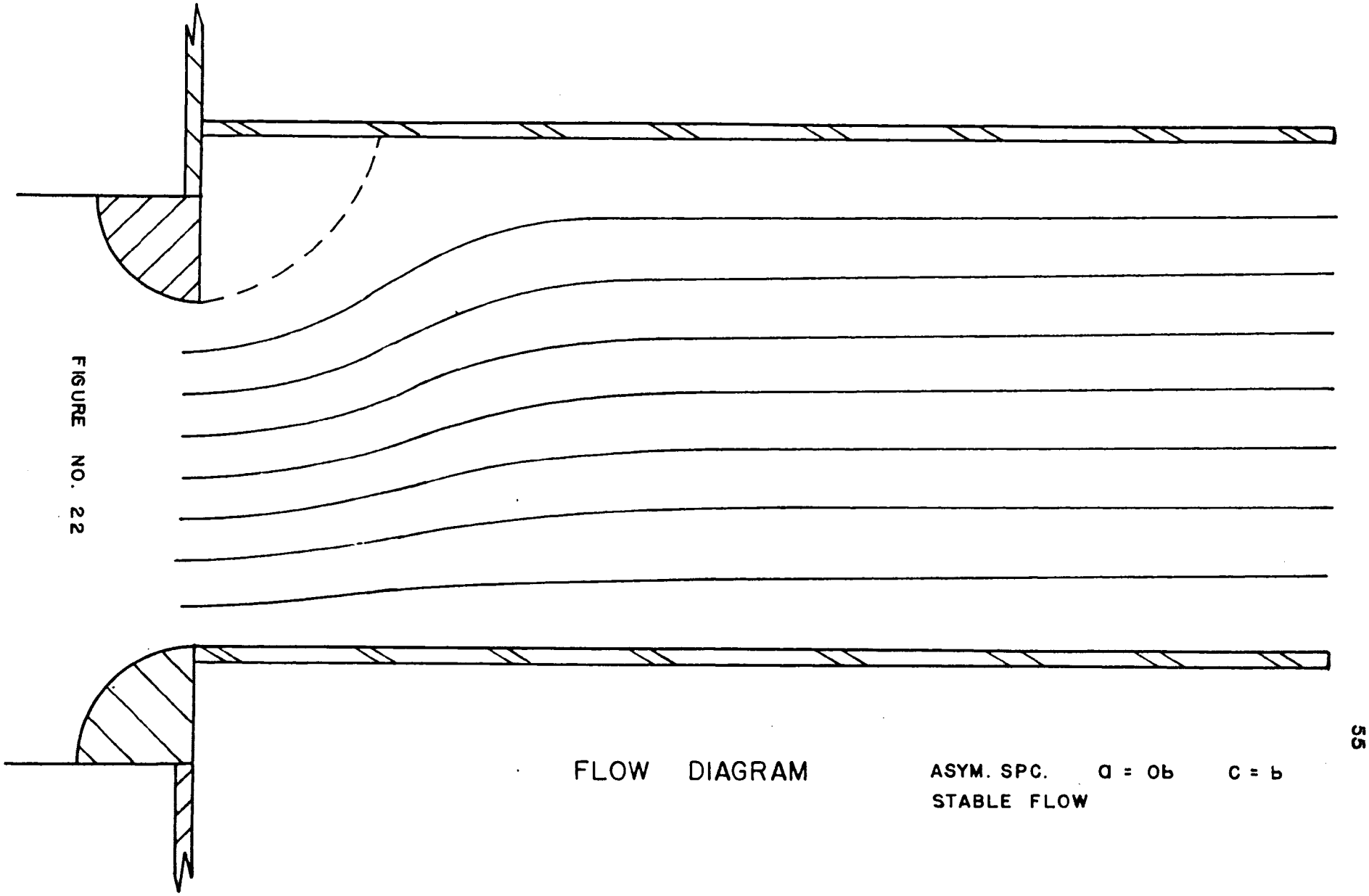

FIGURE NO. 22

FLOW DIAGRAM

ASYM. SPC. a = 0b c = b
STABLE FLOW

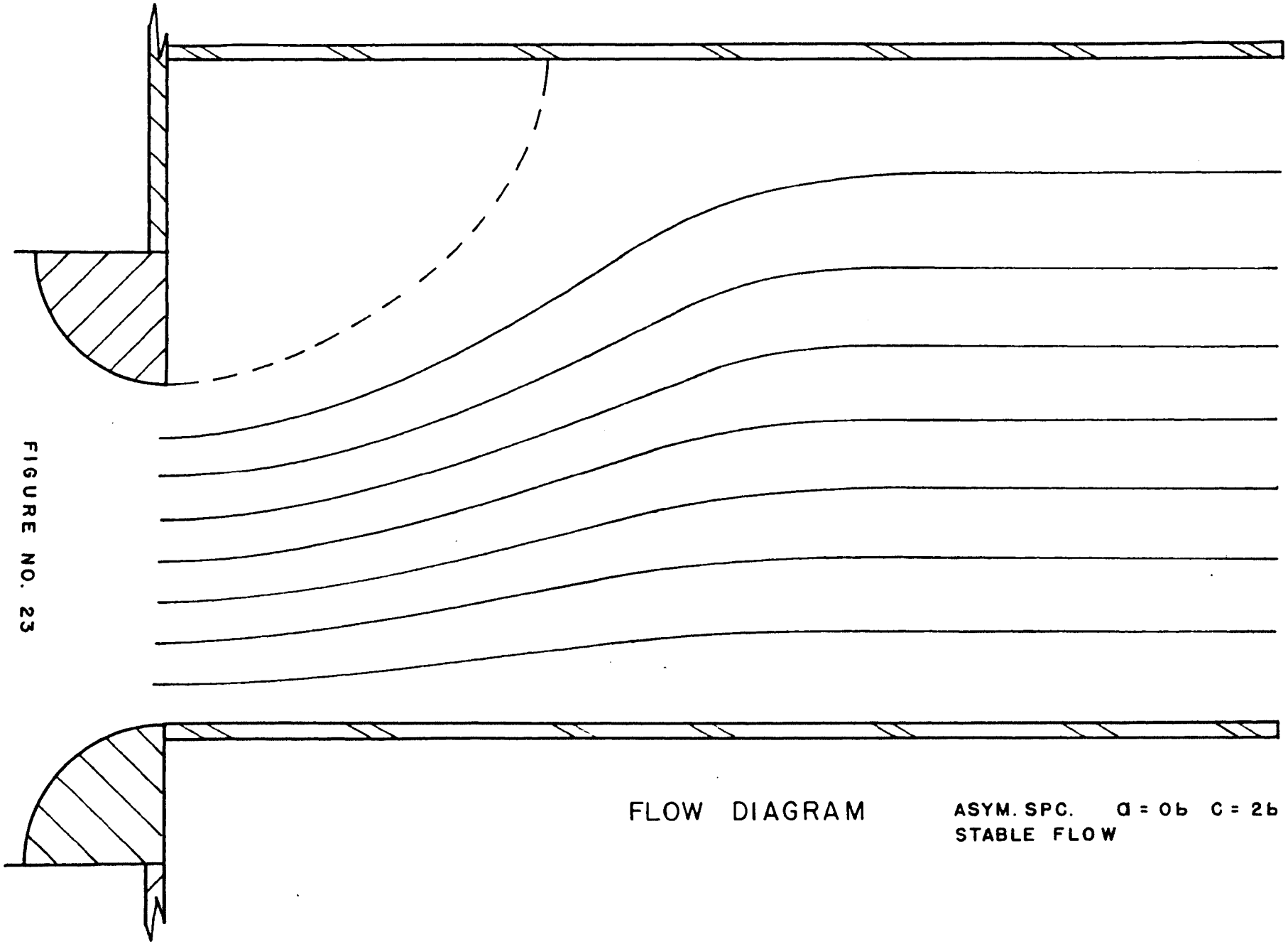

FIGURE NO. 23

FLOW DIAGRAM

ASYM. SPC. a = 0b c = 2b
STABLE FLOW

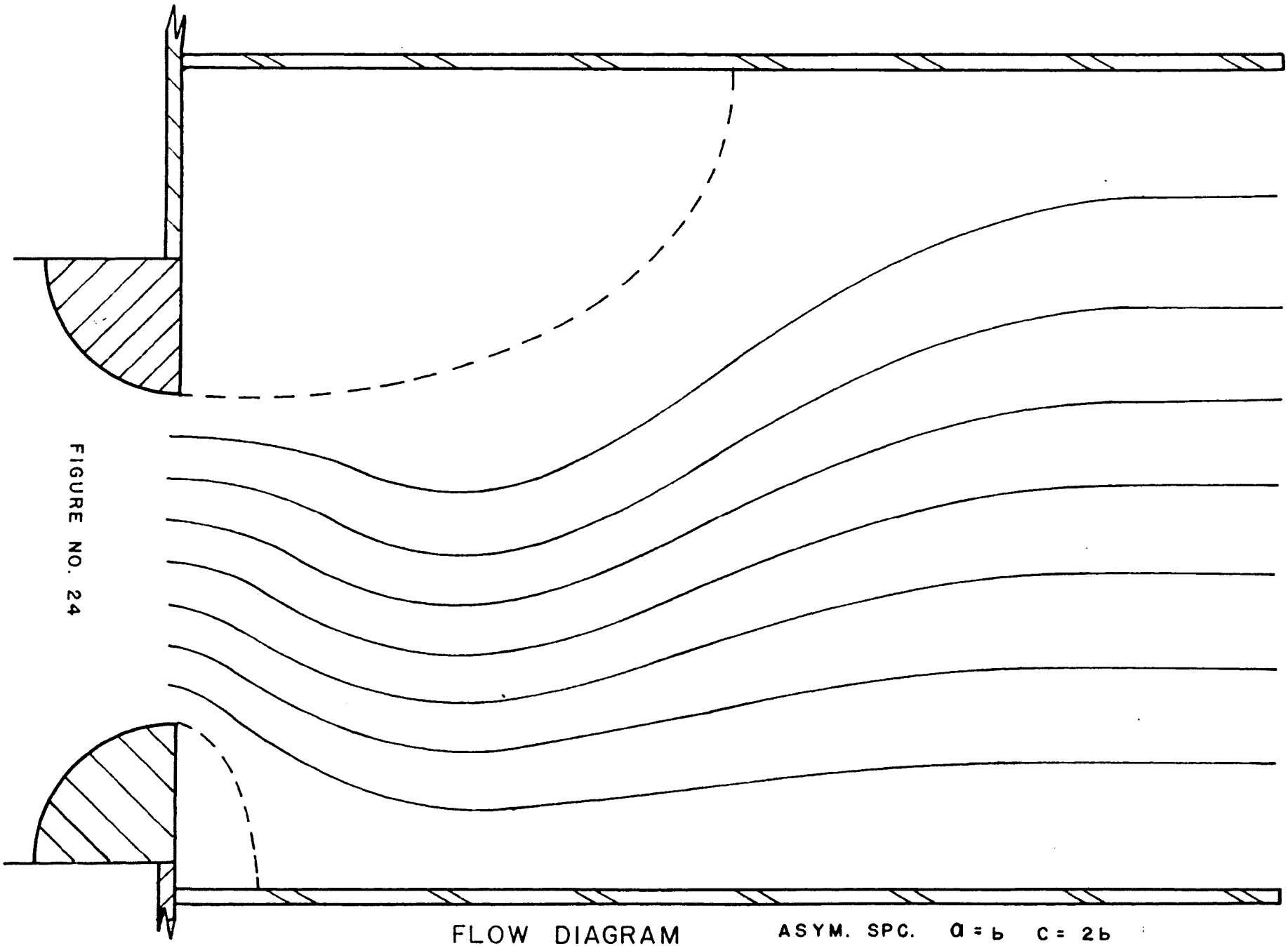

FIGURE NO. 24

FLOW DIAGRAM ASYM. SPC. a = b c = 2b
STABLE FLOW

SEPARATION POCKETS AND THEIR LOCATIONS

ON THE FLOOR AND ROOF OF THE EXPANSION

$\beta = 3b$

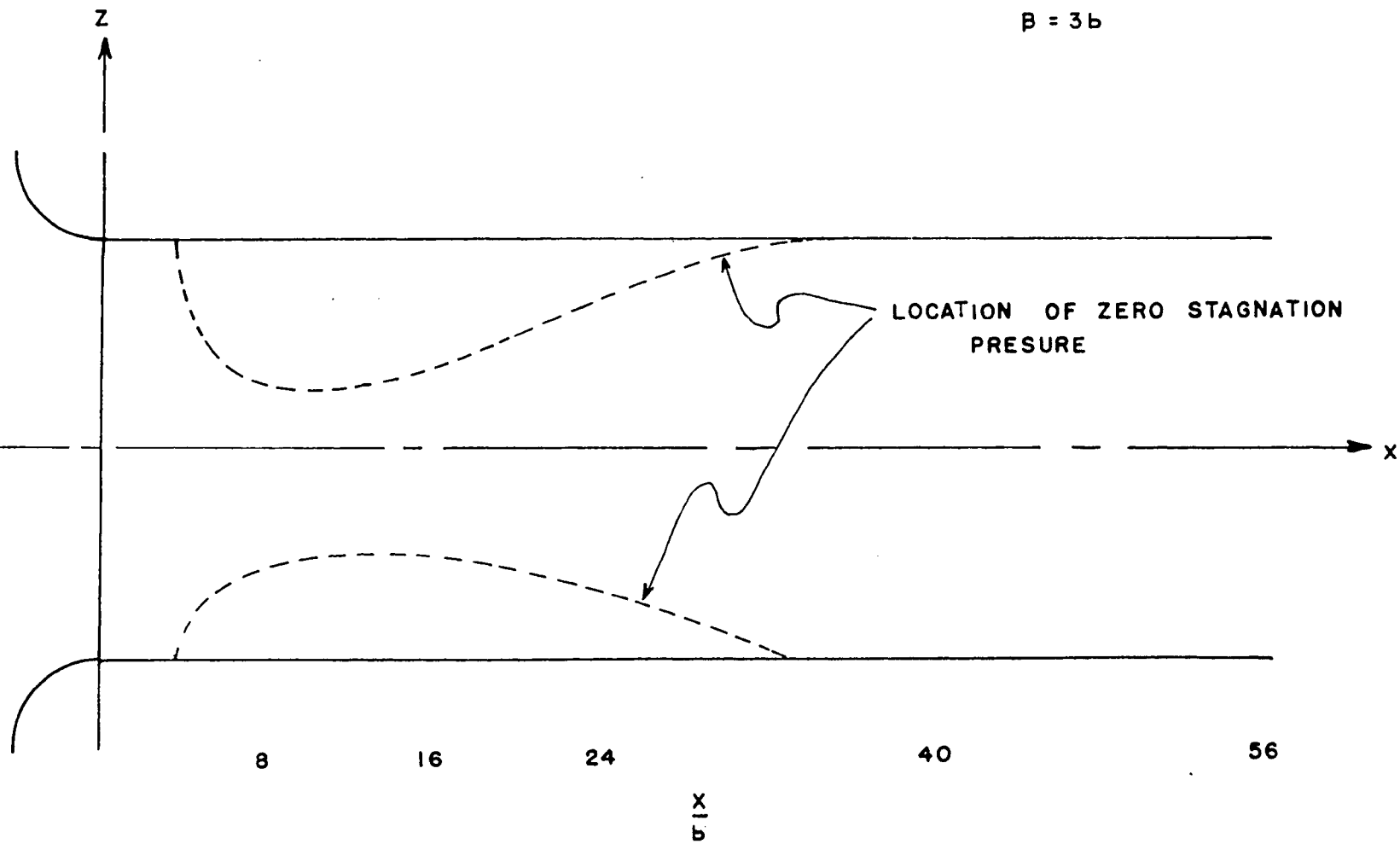

FIGURE NO. 25

REFERENCES

1) H. Rouse, editor, Advanced Mechanics of Fluids, New York, N. Y., 1959, pp. 267-271.

2) Ibid., pp. 271-272.

3) Ibid., pp. 272-275.

4) H. R. Muller, "A Study of the Dynamic Features of a Wall Reattachment Fluid Amplifier," Journal of Basic Engineering, Transactions of the ASME, vol. 86, no. 64 FE 10, Dec., 1964.

5) M. L. Albertson, Y. B. Dai, R. A. Jensen, and Hunter Rouse, "Diffusion of Submerged Jets," Transactions, ASCE, vol. 115, no. 2410, 1950, pp. 639-697.

6) Rouse, op. cit., pp. 272-275.

7) Edward Silberman, discussion of: Turbulence Characteristics of the Hydraulic Jump by H. Rouse, T. T. Siao, S. Nagarathan (Proc., Paper 1528, Feb. 1958), Journal of Hydraulics Division, Proc. ASCE, vol. 84, no. HY3, June, 1958.

8) T. Carmody, "Establishment of the Wake Behind a Disk," Journal of Basic Engineering, Transactions of the ASME, vol. 86, no. 64 FE 3, Dec., 1964.

REFERENCES--Continued

9) J. Laufer, "The Structure of Turbulence in Fully Developed Pipe Flow," N. A. C. A. Report 1174, 1954.